Characterization of the mechanism of
4-Hydroxy-3-methylbut-2-enyl diphosphate reductase (IspH)

by

Xiao Xiao

A thesis submitted to the Graduate Faculty of
Auburn University
in partial fulfillment of the
requirements for the Degree of
Master of Science

Auburn, Alabama
December 14th

Key words: DOXP pathway, IspH, iron-sulfur cluster,
cluster content, freeze quench, EPR measurement

Approved by

Eduardus Duin, Chair, Associate Professor, Chemistry and Biochemistry Department
Douglas Goodwin, Associate Professor, Chemistry and Biochemistry Department
Holly Ellis, Associate Professor, Chemistry and Biochemistry Department

Abstract

In this thesis, two projects were carried in the context of understanding the reaction mechanism of 4-Hydroxy-3-methylbut-2-enyl diphosphate reductase (also called HMBPP reductase or IspH).

The first project is the optimization of the IspH cluster content. It was found that the enzyme activity has a linear relationship with the [4Fe-4S] cluster content. In this thesis, IspH from 3 different organisms: *Aquifex aeolicus, Plasmodium falciparum* and *Escherichia coli* were co-expressed with either the *isc* genes or the *erpA* gene. In the case of the *Plasmodium* enzyme a higher cluster content was observed under both conditions while the *Aquifex* enzyme only showed improvement with the co-expression of the ErpA protein. In the case of the *Escherichia* enzyme the highest cluster content (70%) was found when IspH was expressed all by itself. It is not clear why the co-expression did not work properly.

The second project involved the study of the Escherichia and Aquifex enzymes under pre- and steady state conditions using an EPR-detected freeze-quench method. Both reaction intermediates and possible product signals could be detected. However, the assignment is not straightforward since different electron donors were used in the standard colorimetric assays to obtain the kinetic parameters and the freeze-quench studies to study the formation of paramagnetic reaction intermediates. Future mass spectrometry studies are needed to confirm the assignment of the observed species as reaction intermediates or product-induced signals.

Acknowledgments

This thesis could never be done without the generous help from my utterly wise and patient advisor Dr. Evert Duin. I give him my greatest gratitude. His knowledge and the work ethics taught how to deal with problems and learn from it with calmness and a rational mind. His nice, diligent, and hopeful attitude towards everything influenced me to become a more confident person.

And I also thank my committee members: Dr. Douglas Goodwin, and Dr. Holly Ellis, for there very helpful guidance, as well as their kindness.

I am so thankful for the help, company, understanding, support, and laughter provided by my lab mates Divya Prakash, and Selamawit Ghebreamlak.

Table of Contents

List of Tables

List of Figures

List of Abbreviations

HMBPP	4-Hydroxy-3-methylbut-2-enyl diphosphate
IspH	HMBPP synthases
IPP	Isopentenyl pyrophosphate
DMAPP	Dimethylallyl diphosphate
MVA	Mevalonate
MEP	2-C-methyl-D-erythritol 4-phosphate
DOXP	1-deoxy-D-xylulose-5-phosphate
HiPIPs	High potential Iron-Sulfur proteins
EPR	Electron paramagnetic resonance spectroscopy
MV	Methyl viologen
DIT	Dithionite
CW	Continuous wave
SDS-PAGE	Sodium dodecyl sulfate-polyacrylamide gel electrophoresis
E. coli	*Escherichia coli*
A. a	*Aquifex aeolicus*
P. f	*Plasmodium falciparum*
WT	Wild-Type
n.d.	not detected

Chapter 1: Introduction

1.1. Isoprenoids

Isoprenoids, also called terpenoids, are naturally formed ubiquitous chemical compounds derived from the five-carbon compound isoprene (Figure 1-1), and assembled in thousands of different ways. More than fifty-five thousand isoprenoids have been discovered so far, including carotenoids, cholesterol, rubber, and dolichols (Figure 1-2). They serve a broad variety of functions.

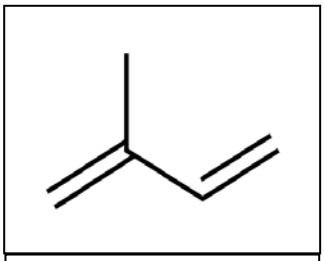

Figure 1-1 Isoprene

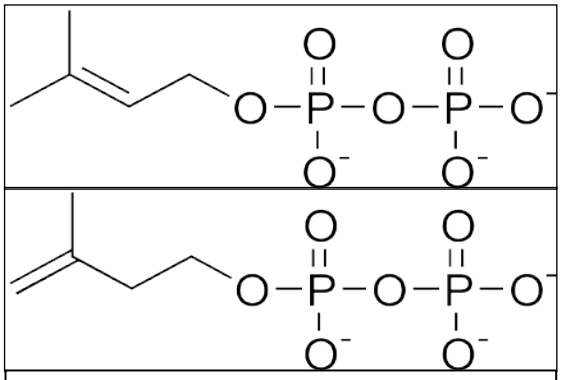

Figure 1-3 IPP and DMAPP

But these isoprenoids compounds do not arise from isoprene itself. Isopentenyl diphosphate (IPP) and dimethylallyl diphosphate (DMAPP) (Figure 1-3) are the natural precursors in biological system to generate the five-carbon isoprene skeleton for isoprenoids synthesis.

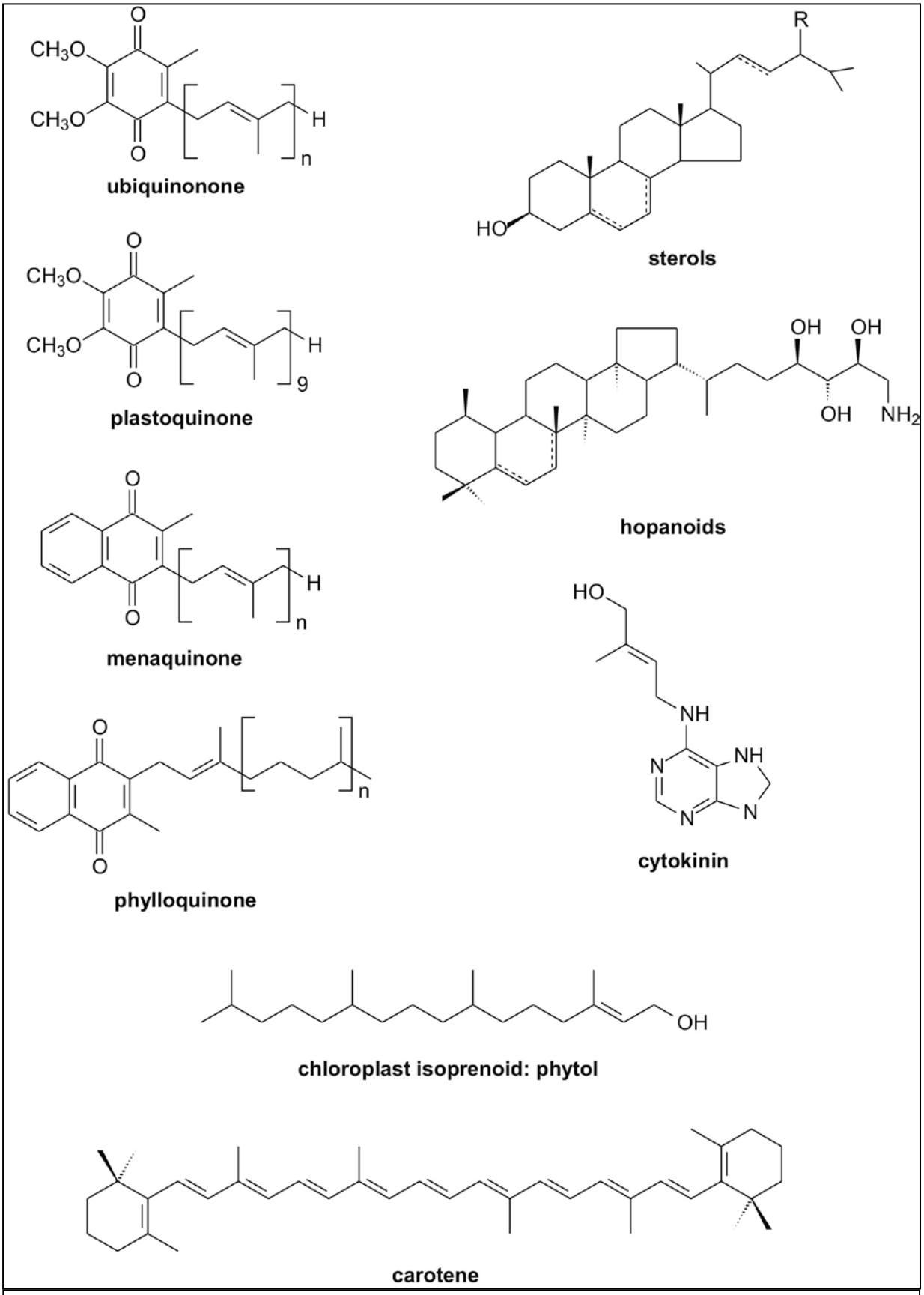

Figure 1-2 Examples of isoprenoids

1.2. Biosynthesis of IPP and DMAPP

1.2.1. Mevalonate (MVA) Pathway

There are two metabolic pathways for the synthesis of these two building blocks. The first well-known biosynthesis of IPP and DMAPP is via the mevalonate (MVA) pathway discovered in the 1950s (1), and it has been well documented in eukaryotes through the pioneering work of Bloch, Lynen and Cornforth in the 1980s (2-4). This pathway, the only pathway present in animals, fungi, and certain bacteria, produces both IPP and DMAPP and takes place in the cytosol. The complete pathway is shown in Figure 1-4. The pathway begins with 2 acetyl-CoA, molecules which undergo a condensation catalyzed by thiolase to form acetoacetyl-CoA. Then a third acetyl-CoA condenses with this acetoacetyl-CoA to generate 3-hydroxy-3-methylglutaryl-CoA (HMG-CoA) via HMG-CoA synthase. NADP-dependent HMG-CoA reductase catalyzes the conversion of HMG-CoA to mevalonate (MVA) and a CoA-SH. Mevalonate 5-phosphotransferase transfers a phosphoryl moiety to MVA with the generation of 5-phosphomevalonate (also called phosphomevalonic acid). Then this phosphomevalonic acid obtains another phosphoryl moiety and converts into 5-pyrophosphatemevalonate (also called M-5-P), catalyzed by phosphomevalonate kinase. Pyrophosphate mevalonate decarboxylase yet brings in a third phosphoryl moiety to M-5-P which destabilizes the terminal carboxyl group. The resulting decarboxylation and dephosphocytidylation generates the product isopentenyl pyrophosphate (IPP). Finally, IPP isomerase converts IPP to its isomer dimethylallyl diphosphate (DMAPP).

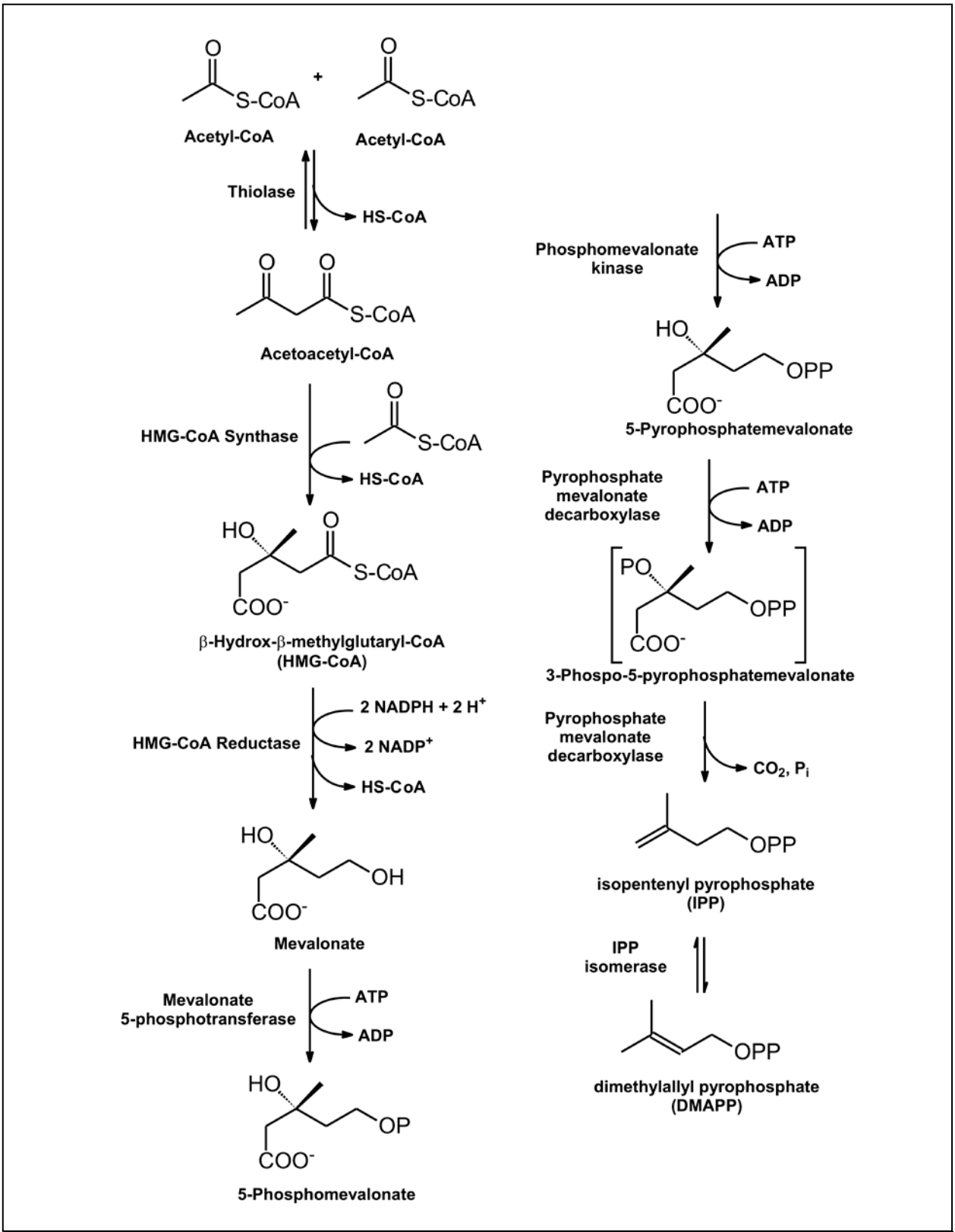

Figure 1-4 Mevalonate pathway

1.2.2. MEP/DOXP pathway

An alternative biosynthesis pathway for isoprene units, the non-mevalonate pathway (Figure 1-5) was discovered in the late 1980s (5-7) by Rohmer. It functions in chloroplasts, algae, cyanobacteria, apicomplexan parasites, and many other eubacteria. This pathway starts with the condensation of pyruvate with D-Glyceraldehyde-3-phosphate (G3P) to form the carbon skeleton 1-Deoxy-D-xylulose 5-phosphate (DOXP) catalyzed by DOXP synthase (DXS). The linear carbon skeleton of DOXP requires a skeletal rearrangement to generate the branched chain 2-C-Methyl-D-erythritol-4-phosphate (MEP), catalyzed by DOXP reductoisomerase (also named IspC). MEP cytidylyltransferase (also named IspD) catalyzes the transfer of a phosphoryl moiety to MEP with the formation of 4-Diphosphocytidyl-2-C-methyl-D-erythritol (CDP-ME). Then CDP-ME kinase (also named IspE) phosphorylates the C_2-hydroxyl group of CDP-ME forming 4-diphosphocytidyl-2-C-methyl-D-erythritol 2-phosphate (CDP-MEP) through release of CMP by the catalytic action of MEcPP synthase (also named IspF), a cyclic diphosphate 2-C-methyl-D-erythritol-2,4-cyclopyrophosphate (MEcPP) was generated. HMBPP synthase (IspG or GcpE) catalyzes the ring opening step of MEcPP with the formation of (*E*)-4-hydroxy-3-methyl-but-2-enyl pyrophosphate (HMBPP). Finally, HMBPP obtains two electron equivalents, resulting in the cleavage of a nonactivated C-OH bond, resulting in the formation of either isopentenyl pyrophosphate (IPP) or dimethylallyl pyrophosphate (DMAPP). This last step is catalyzed by HMBPP reductase (IspH or LytB).

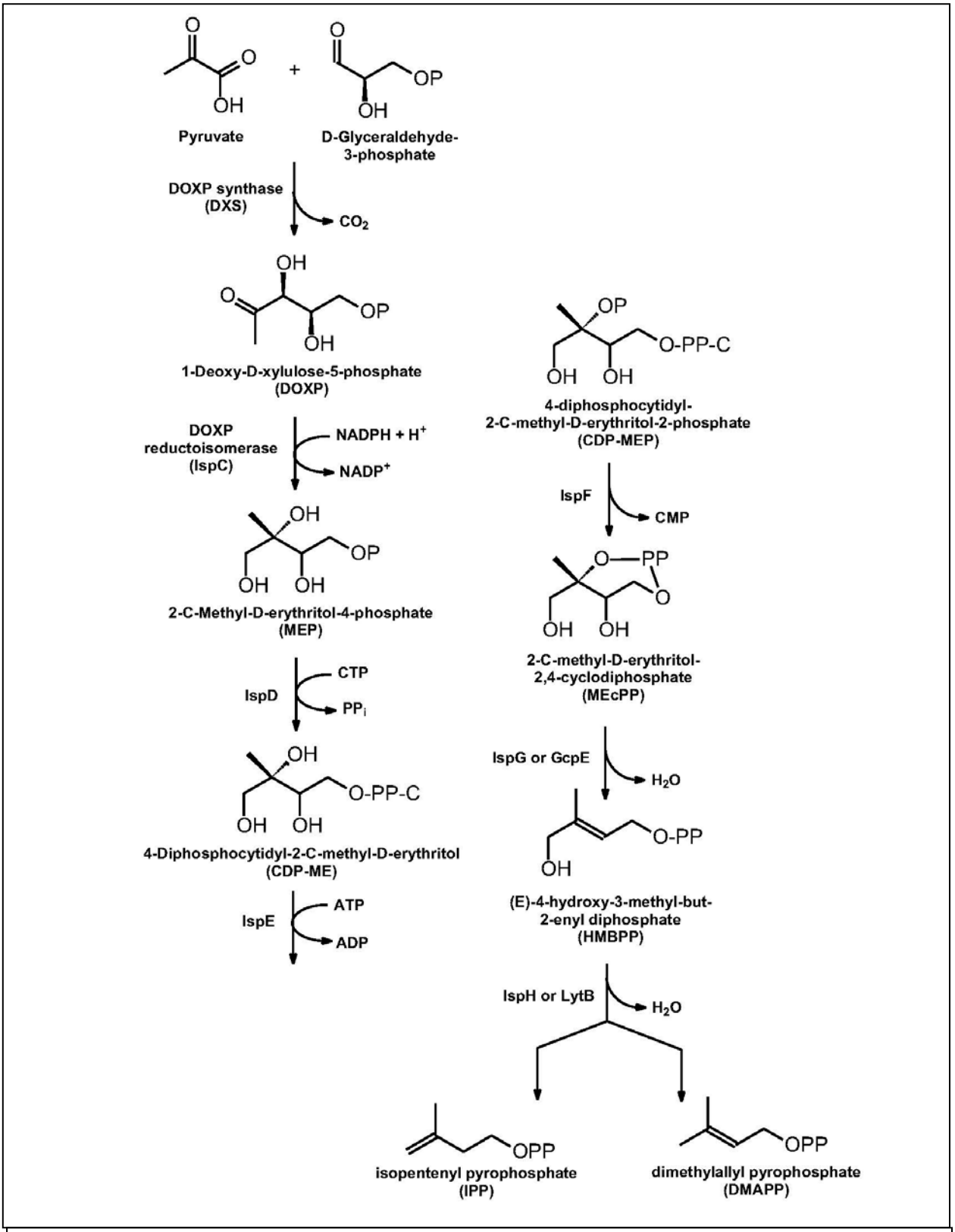

Figure 1-5 DOXP/MEP pathway

1.2.3. Research purpose

In both pathways, IPP and DMAPP are the end-products and the precursors of isoprenoids. These two pathways are mutually exclusive in most organisms, but in plants and a few bacterial species they are both present and functional. The fact that the MEP/DOXP pathway does not exist in humans makes it a promising target for the design of drugs to kill pathogens that use the MEP/DOXP pathway as its main source to produce IPP and DMAPP.

Except for the last two enzymes of the MEP/DOXP pathway, IspG and IspH, the reaction mechanisms of the other enzymes have been studied and described thoroughly. The goal of the research in the Duin group is to elucidate the reaction mechanisms of IspG and IspH.

Here we will only focus on the last enzyme, IspH, with the aim of understanding the mechanism and to design an effective antibiotic drug. The first stage, however, is to obtain information about possible intermediates in the reaction pathway already detected, and establish their catalytic competence.

Shown in Figure 1-6 is the structure of the active site of IspH from *Escherichia coli* detected in crystals of the enzyme cocrystalized with the substrate HMBPP (8). The active site [4Fe-4S] cluster is in silver and yellow. Three of the iron ions of the cluster are coordinated to the enzyme by three cysteine residues.

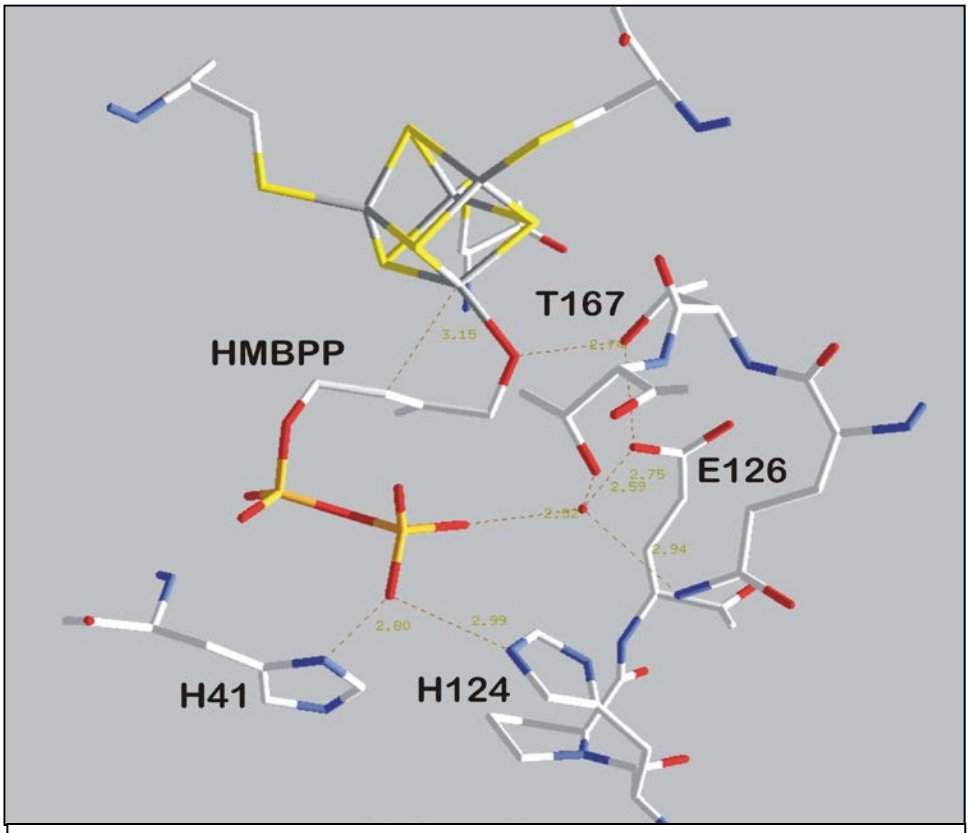

Figure 1-6 Active site of IspH from E. coli cocrystalized with HMBPP

The fourth iron, also called the unique iron, is normally only bound by three sulfur ions from the cluster itself. In the crystal structure, however, HMBPP forms the fourth ligand and is bound to the cluster via its hydroxyl group. The binding of HMBPP in the active site is further stabilized by a network of hydrogen bonds involving Tyr167, Glu126, and a water molecule. In addition, the pyrophosphate group of HMBPP is coordinated to 2 histidine residues: His42 and His124. Site directed mutagenesis of residues His42, His124 and Glu126 and subsequent kinetic and spectroscopic characterization of the mutant enzyme confirmed the importance of the residues in binding HMBPP and their proposed role in the catalytic mechanism (9-11).

1.3. Iron-Sulfur Clusters

1.3.1. Introduction

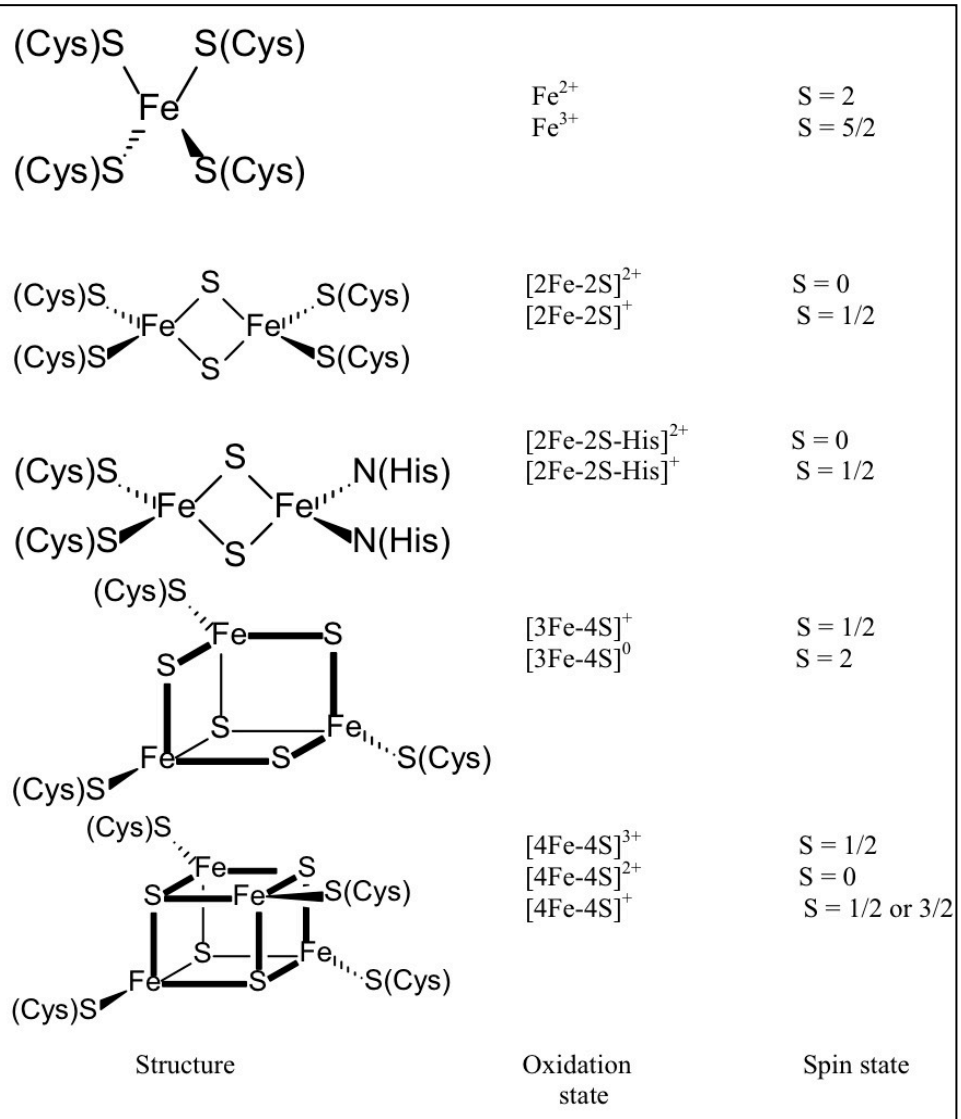

Figure 1-7 Different forms of iron-sulfur clusters, such as Fe_2S_2, Fe_3S_4, and Fe_4S_4 clusters and so on, with different charges and spin states.

Many proteins need a cofactor for their catalytic functions. There are organic cofactors like nucleotides and vitamins, metallo-organic cofactors, as well as inorganic cofactors, with various metal ions. Iron and sulfur were two of the most abundant environmental elements on ancient earth. Iron-sulfur-cluster-containing proteins are found in all life forms. Fe-S clusters were discovered in the early 1960s. These Fe-S proteins included ferredoxins from plants and bacteria, and the respiratory complexes I-III of bacteria and mitochondria. There is a whole range of different types of iron-sulfur clusters that can contain 2, 3, 4, 7, or 8 iron atoms.

Some of these are shown in Figure 1-7. They display different midpoint potentials (Figure 1-8), as well as different spectra in EPR spectroscopy (Figure 1-9). These clusters can undergo oxidation-reduction reactions. To study these iron-sulfur proteins, protein samples either oxidized with ferricyanide or reduced with dithionite are prepared. The obtained signals can be compared with the typical EPR signals displayed in Figure 1-9.

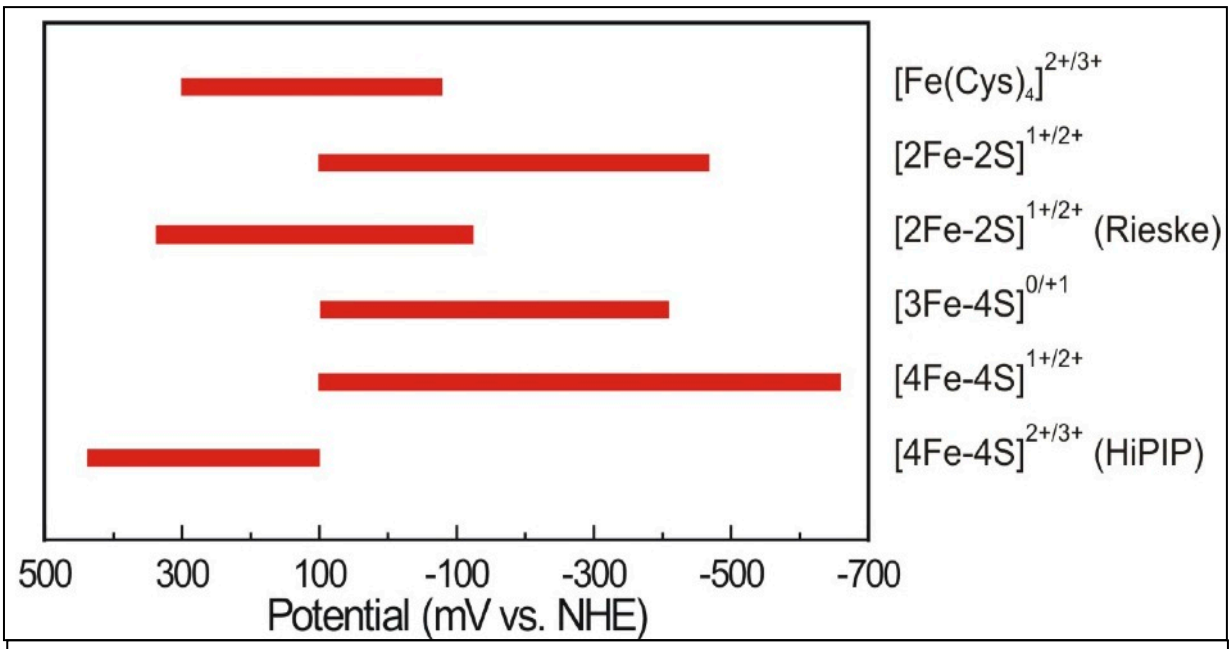

Figure 1-8 Range of redox potentials for different types of iron-sulfur clusters.

Malkin and Rabinowitz developed reconstitution protocols in 1966 to put Fe-S clusters back into the apoproteins *in vitro* (4), suggesting that these cofactors can be spontaneously assembled. In the presence of isotope, ^{57}Fe and/or ^{35}S, it has been observed that these are inserted into the core cluster using NMR spectroscopy. However, studies in the 1990s (15) showed that the maturation of Fe-S proteins is a catalytic process rather than a spontaneous one. Before going into detail about that process let us first look at the diversity in function of Fe-S clusters and cluster-containing proteins and enzymes.

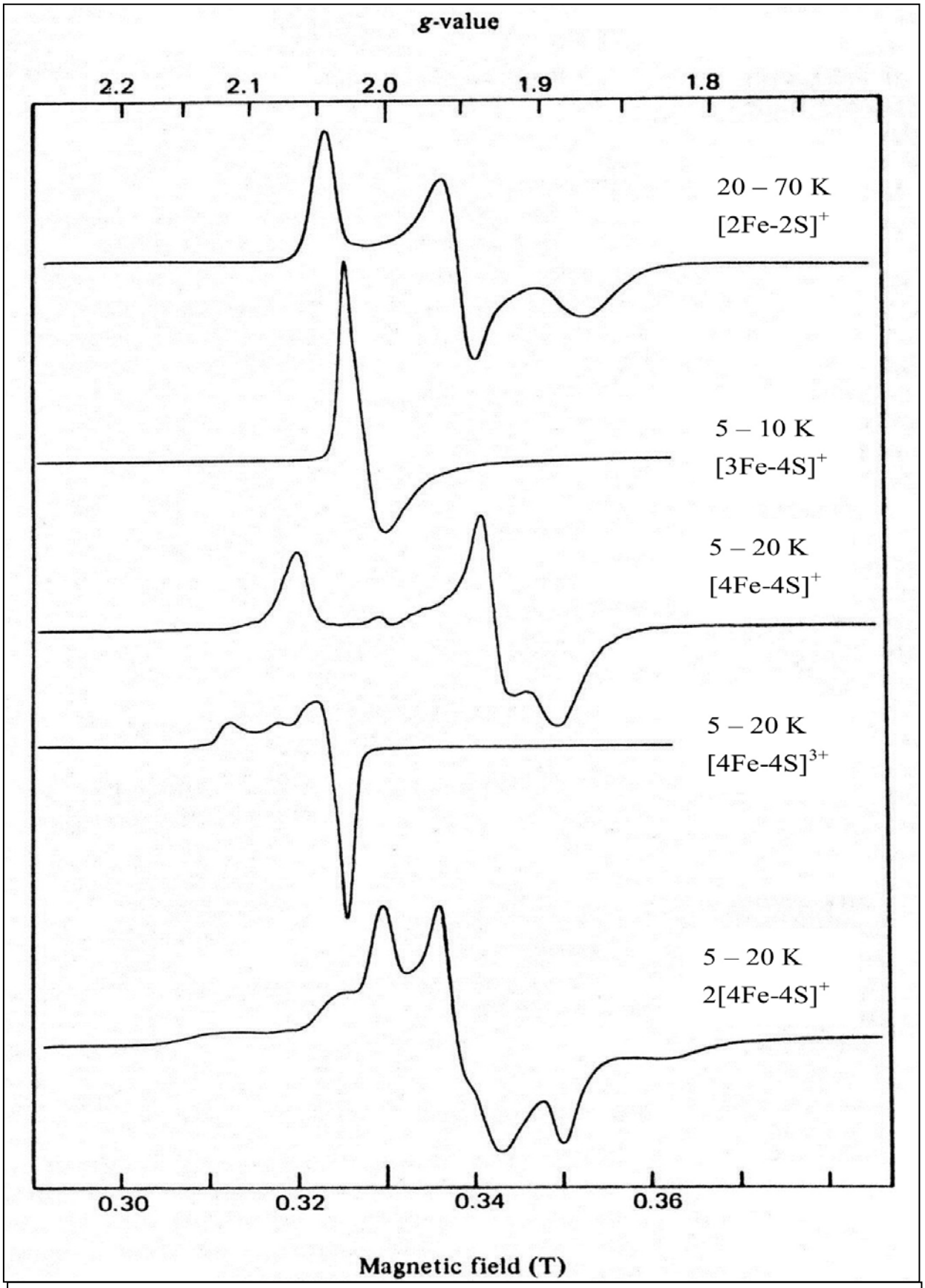

Figure 1-9 Different clusters also have different EPR spectra

1.3.2. Function

1.3.2.1. Electron transfer

The most common function of iron-sulfur clusters is in electron transfer, since the Fe has the ability to switch between the 2+ and 3+ oxidative states (16). Given the proteinaceous surrounding, iron-sulfur clusters can adopt redox potential from -500mV to +300 mV (Figure 1-8) (17). With this wide range, iron-sulfur clusters can serve as good electron donors and acceptors, and as biological electron transport mediators. They are very important components in photosynthesis and respiratory processes. For example, ferredoxins form one of the largest classes of biological electron carriers. Most of the iron-sulfur clusters are one-electron carriers, except the double cubane [7Fe-8S] cluster found in nitrogenases which can function as a two-electron carrier.

1.3.2.2. Substrate binding and activating

Another well-studied function of Fe-S clusters is in catalysis. Aconitase is highlighted here as an example (Figure 1-10). The enzyme contains an active-site [4Fe-4S] cluster, which catalyzes first a dehydration followed by a rehydration reaction to convert citrate via cis-aconitate into isocitrate in the citric acid cycle. When substrate binds to the unique uncoordinated iron, the ion becomes hexacoordinated. Coordination to the unique iron ion makes the C_3 hydroxyl group a better leaving group. This abstraction results in the formation of a double bond, which is the intermediate cis-aconitate. Then the intermediate goes through a 180° "flip" around the carbon

double (C=C) bond resulting in the coordination of the carboxyl group present at the other end of the molecule. The hydroxyl group affected the nearer carbon of the C=C double bond results in the formation of isocitrate. In this case, the iron-sulfur cluster only acts as a binding site for the substrate. No redox chemistry is involved in the transformation of citrate into isocitrate.

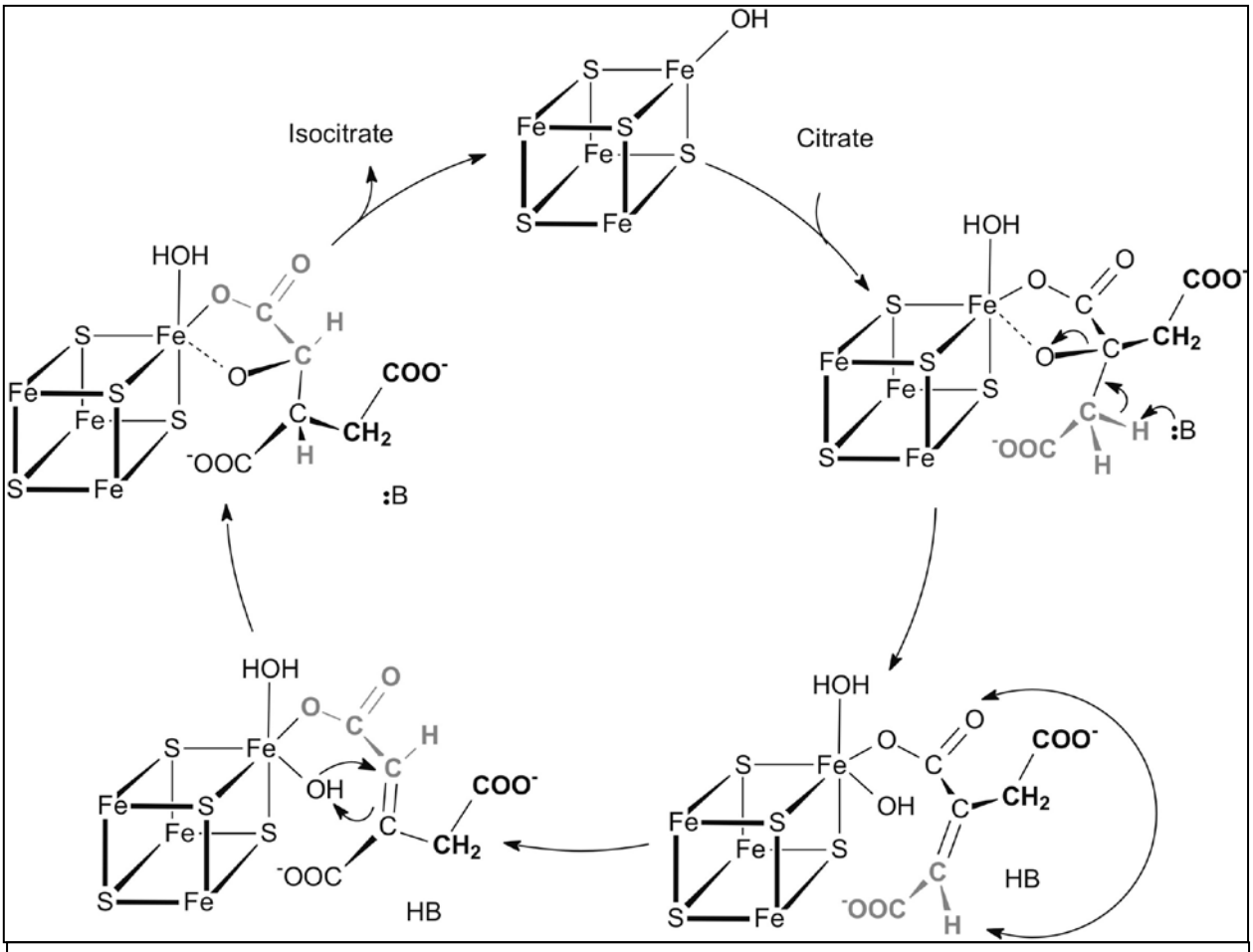

Figure 1-10 Reaction mechanism of aconitase

Another example is formed by the radical SAM enzymes (Figure 1-11) (18). In this case, the [4Fe-4S] cluster is involved in substrate binding as well as electron transfer. The binding of S-Adenosyl methionine (SAM) is via its carboxyl oxygen and the nitrogen from the amino group. The binding is followed by donation of an electron to the sulfonium sulfur atom which result in breaking of the S-C bond generating a cluster bound methionine and a radical species, 5'-

deoxyadensyl. This species can abstract a hydrogen atom from another molecule such as an organic substrate or amino acid to form other radical species.

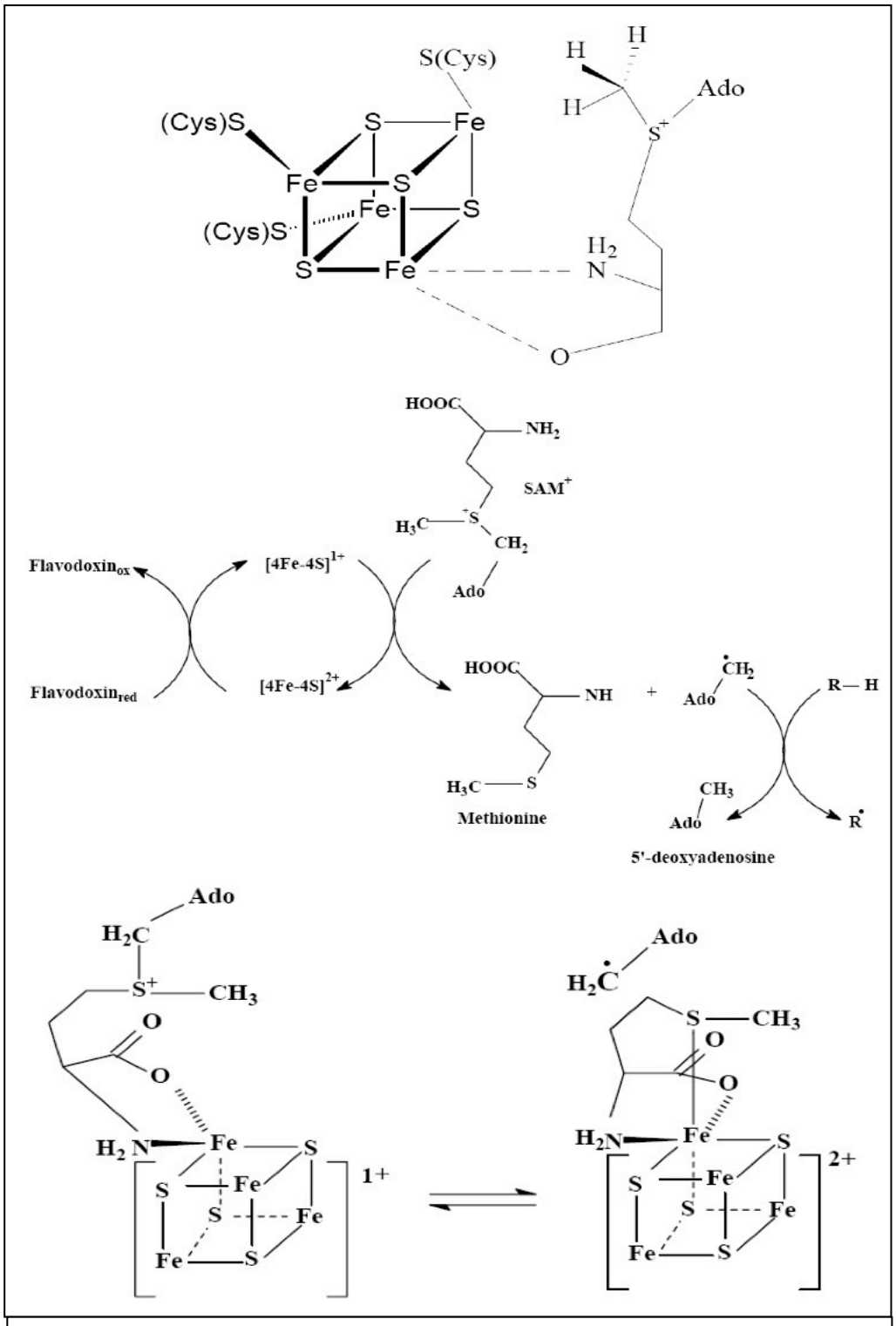

Figure 1-11 Reaction mechanism of radical SAM enzymes

1.3.2.3. Regulatory and sensing function and other functions

A third general function of Fe-S clusters is in sensing the environment or intracellular conditions in coordination with the regulation of gene expression. For example, mammalian cytosolic iron regulatory protein 1 (IRP1) under iron-abundant conditions contains a [4Fe-4S] cluster and function as an aconitase. Under iron deprivation conditions, however, the cluster is lost and now the enzyme is able to bind to DNA and regulate the synthesis of proteins involved in iron uptake. (19)

Function Cluster type	Cluster type	Examples
Electron transfer	[2Fe-2S]; [3Fe-4S]; [4Fe-4S]	Ferredoxins; redox enzymes
Coupled electron/proton transfer	[2Fe-2S]	Rieske protein
Substrate binding and activation	[8Fe-7S]	Nitrogenase
	[4Fe-4S]	(de)Hydratases
	[4Fe-4S]	Radical SAM enzymes
	Ni-Ni-[4Fe-4S],[Ni-4Fe-5S]	Acetyl-CoA synthase
	[4Fe-4S]-siroheme	Sulfite reductase
Fe or cluster storage	[4Fe-4S]	Ferredoxins
	[4Fe-4S]	Polyferredoxins
	[4Fe-4S]	Structural Endonuclease III
	[4Fe-4S]	MutY
Regulation of gene expression	[2Fe-2S]	SoxR
	[4Fe-4S]/[2Fe-2S]	FNR
	[4Fe-4S]	IRP
	[2Fe-2S]	IscR
Regulation of enzyme activity	[4Fe-4S]	Glutamine PRPP amidotransferase
	[2Fe-2S]	Ferrochelatase
Disulfide reduction	[4Fe-4S]	Ferredoxin:thioredoxin reductase
	[4Fe-4S]	Heterodisulfide reductase
Sulfur donor	[2Fe-2S]	Biotin synthase

Table 1-1Iron-sulfur cluster have wide range of functions. Adapted from (20)

Fe-S proteins have other functions like the storage (and donation) of iron and sulfur ions, and oxygen sensing. These functions are listed in table 1-1. (20)

1.3.3. Biogenesis of iron-sulfur clusters

1.3.3.1. Biogenesis systems

Studies of the maturation of bacterial Fe-S clusters performed with *Escherichia coli*, azototrophic (nitrogen-fixing) *Azotobacter vinelandii*, and yeast *Saccharomyces cerevisiae* have identified three major systems for the biosynthesis of Fe-S proteins. The NIF system is responsible for the clusters in the enzyme nitrogenase. The ISC and SUF are more general, and they are responsible for generating Fe-S clusters under normal and oxidative-stress conditions, respectively. The ISC system that functions in the mitochondria is homologous to that found in bacteria. In addition, the CIA machinery for Fe-S biosynthesis functions in the cytosol and the nucleus of eukaryotes. Despite the differences among the various discovered systems in different organisms, they all follow the same basic steps for cluster synthesis.

There are two main steps in the generation of an Fe-S protein *in vivo*: First there is the assembly of the Fe-S cluster on a scaffold protein. Second, the complete cluster is transferred to an apoprotein. Typically five different types of proteins are involved in these processes (Figure 1-12): (1) Sulfur donor. A cysteine desulfurase that removes a sulfur ion from cysteine to produce a persulfide on one of its own cysteine residues (NifS, IscS, SufS in bacteria, and Nfs1-Isd11 in mitochondria). This sulfur is used to donate to the new cluster. (2) Iron donor. Although the

origin of iron is not completely understood, studies suggested the CyaY enzyme in bacteria, Yfh1 in mitochondria, and Frataxin in Mammals can bind iron and transfer it to the scaffold protein. (3) Electron transfer. Sulfur S^0 (persulfide on the desulfurase) need to be transferred and converted to sulfide S^{2-} to be able to be used as an Fe-S cluster building block. This job is probably done by a ferredoxin reductase in combination with a ferredoxin in the ISC system or by the ferredoxin-like domain of NifU in the NIF system. (4) Scaffold proteins. Examples are IscU, SufU and NifU in bacteria, Isu1 in eukaryote, IscA and SufA in plasmids. They contain conserved cysteine residues that constitute the building site where a stable structure can be created. (5) Transfer protein, A type carrier (ATC) such as IscA, SufA. After the Fe-S cluster is assembled, it will be dissociated from the scaffold by chaperon protein (such as HscA and HscB in ISC system, Ssq1 and Jac1 in mitochondria, and Nar1 and Cia1 in CIA machinery) to an ATC, then the ATC will accurately transfer the cluster to the target apoprotein. Although ATCs are not crucial in experiments *in vitro*, they are essential in living cells under various growth conditions. (19)

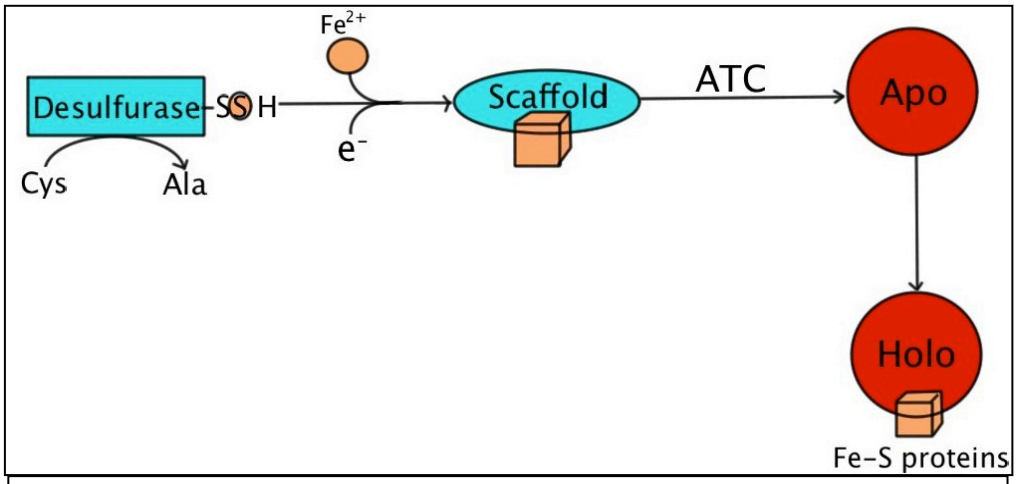

Figure 1-12 Schemmatic representation of the iron-sulfur cluster biogenesis system

For our research project IspH from different sources is overexpressed in an *E. coli* host. To improve the cluster content the enzyme is expressed in a host that also overexpresses the basic set of ISC genes and the IspG/IspH specific gene *erpA.*

1.3.3.2. Biogenesis repair component: ErpA

Due to their redox properties, iron-sulfur clusters are ubiquitous cofactors presented in protein controlled processes like electron transfer, and oxygen sensing. Unfortunately, under some conditions iron-sulfur clusters can be very fragile and hazardous elements (22). They can be easily damaged by exposure to oxygen. This can convert the cluster $[4Fe\text{-}4S]^{2+}$ form to an unstable $[4Fe\text{-}4S]^{3+}$ form that might lose one Fe^{2+} to yield an inactive $[3Fe\text{-}4S]^{1+}$ form. Moreover, the released ferrous iron ion might react with O_2 and H_2O_2 forming reactive oxygen species (ROS) like the hydroxyl radical (·OH) that can damage DNA and membranes. Secondly, ROS can alter the Fe-S clusters biogenesis ISC/SUF systems. The ISC system becomes inactivated by ROS. In this situation the SUF system can still synthesize Fe-S clusters. However, the iron limitation under these stressed conditions would cause the SUF system to insert cobalt or copper as replacements for iron, and generate mixed clusters. Studies have shown that a 1 hour incubation of IscU or SufA with $CoCl_2$, monitored by UV spectrometry, the full-iron signal would decreases, while the mixed-cobalt signal rises correspondently. Indicating IscU or SufA forms mixed iron-cobalt-sulfur clusters. The incubation of these mixed scaffold protein with apo-target protein showed the transfer of the mixed cluster to the apo-protein. Since cysteine residues have much higher affinity for Co^{2+}, the scaffold protein with mixed cluster is much less effective, with more scaffold protein containing mixed cluster, the Fe-S assembling process is

impaired. Only low amount of active holo-protein were generated. In this case, the whole iron-sulfur biogenesis system is poisoned. (23)

On top of the ISC and SUF genes more genes appear to be needed for the synthesis of clusters in specific enzymes and proteins. The maturation of the IspH and IspG enzyme is a good example that shows that the ISC and SUF systems are not sufficient enough for the maturation of the enzymes under all growth conditions. That's the reason we also consider ErpA (essential respiratory protein A), a non-ISC, non-SUF component, for IspG/IspH maturation in presence of oxygen or other electron acceptors (27). Studies have shown that the MVA pathway in eukaryotic cells has a respiratory defect when the *erpA* gene is mutated. ErpA is essential for growth of *E. coli* in the presence of oxygen or alternative electron acceptors. Cell with a mutated *erpA* gene (expression of the gene under arabinose induction and glucose repression), contained a greatly reduced amount of ubiquinones. In addition it was shown

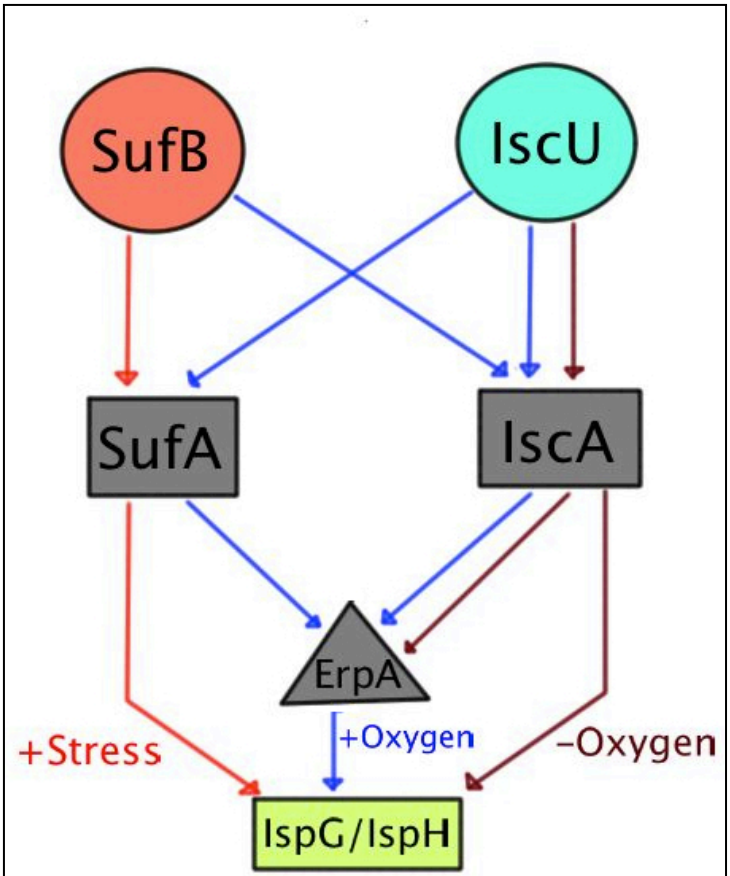

Figure 1-13 ErpA is essential for growth of E. coli in the presence of oxygen or alternative electron acceptors.

that incubation of ErpA with apo-IspG will generate holo-IspG, indicating that ErpA could be essential for the maturation of IspG and also maybe IspH (Figure1-13).

1.4. The Reaction Mechanism of IspH

To be able to design a highly efficient drug, knowledge of the structure of the target enzyme active site is needed, as well as a thorough understood reaction mechanism. The goal would be to find transition state analogs or even better suicide inhibitors that would provide optimal binding to the target enzyme and completely shut it down. Several new paramagnetic species have been detected in kinetic studies. Based on these, however, several different reaction mechanisms have been proposed.

Recently Groll's group (10) co-crystallized IspH from *E. coli* with its substrate HMBPP. The crystal structure (Figure 1-6) showed that the protein contains a [4Fe-4S] cluster. In this structure, 3 irons are coordinated by three conserved cysteine residues (Cys12, Cys96, Cys197), and the fourth iron is coordinated by HMBPP

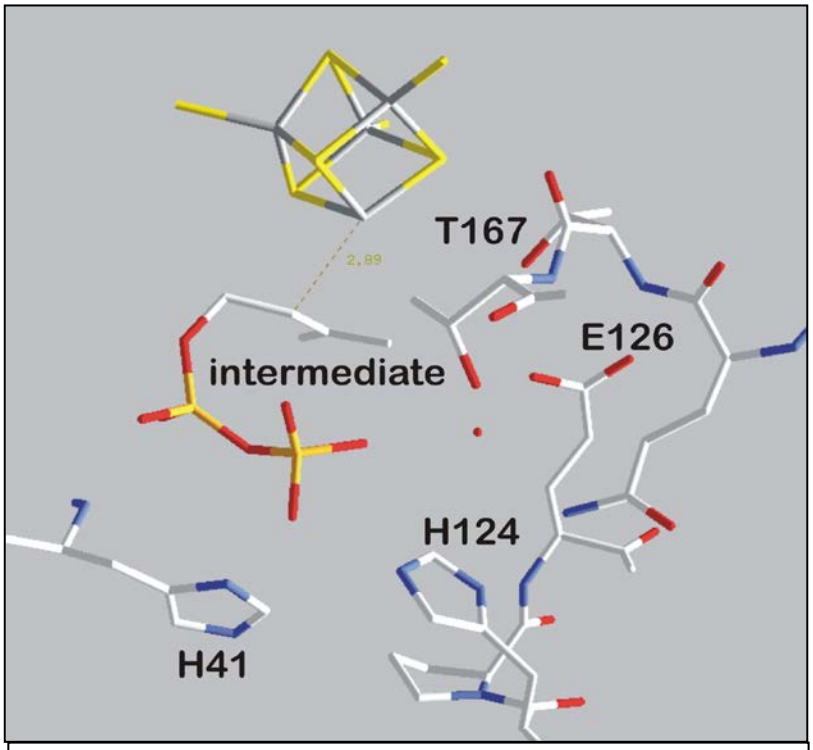

Figure 1-14 Active site of IspH from E. coli cocrystalized with intermediate

through the C_4-OH group. HMBPP has a hairpin conformation; the carbon backbone is sandwiched between the cluster and its own pyrophosphate group. An extensive H-bond network exists between HMBPP, Tyr167, Glu126, and a water molecule present in the active site. The distance between the unique iron and the substrate's olefinic carbons (C_2=C_3) is 2.8-3.0Å, which is shorter than all the van de Waals radii sum together (3.6 Å), but longer than a typical organometallic iron allylic complex (2.0-2.1Å). This would be in line with a direct Fe-O bond.

The crystals turned out to be highly sensitive to X-rays. Extended exposure of the IspH-HMBPP complex to X-rays, assuming that the photons irradiation triggered the formation of solvated electrons, led to the decrease of the distance between the unique iron and the olefinic group, and disappearance of the C_4 alkoxide group (Figure 1-14). The water molecule that should be generated because of the dehydrogenation of the substrate HMBPP was not be detected. One explanation for this may be that this H_2O is highly disordered. Co-crystallization of the enzyme with its product (Figure 1-15), resulted in a structure where the product is bound in an orientation distinct from that of HMBPP. In addition, two water molecules can be observed in the structure.

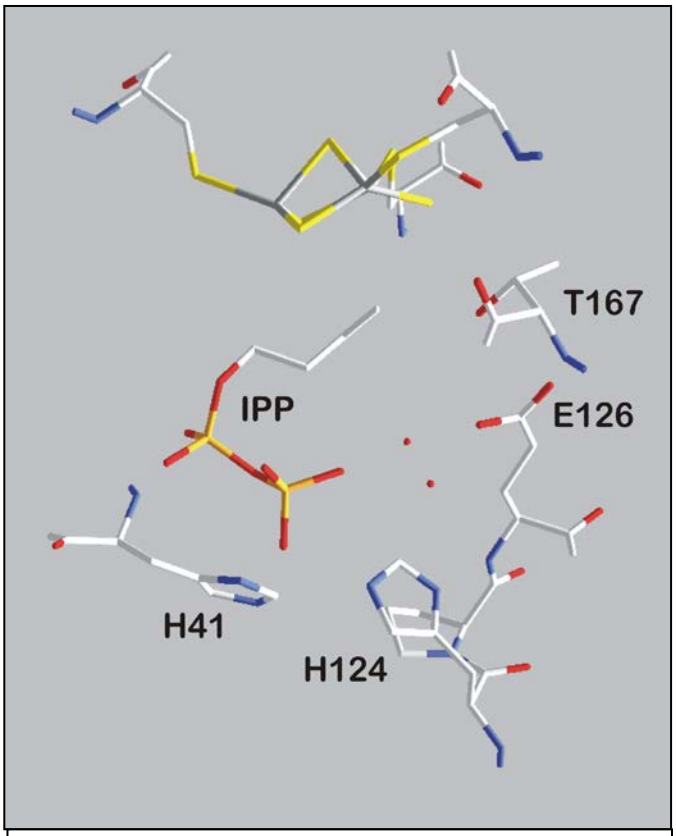

Figure 1-15 Active site of IspH from E. coli cocrystalized with IPP

Based on the information above and other spectroscopic data, several models have been proposed for IspH catalysis during the past two decades, including cationic, anionic, radical, and diene intermediates. The Birch reduction and the bio-organometallic models are two of the more viable mechanisms being considered.

1.4.1. Birch reduction model

A Birch reduction is a mechanism first proposed by the Australian chemist Arthur Birch (1915–1995) in 1944. In this mechanism, the olefinic group of the substrate receives an electron to generate a carbanion and a radical anion, the carbanion then receives a proton, and the radical anion receives another electron and another proton subsequently to finish the reaction.

The reaction (Figure 1-16) (10) initiates by coordination of the C_4-OH to either the oxidized or the reduced [4Fe-4S] cluster through the unique iron site. Electron transfers from the reduced form of the cluster to the substrate results in the formation of a radical anion species. Now the [4Fe-4S] cluster can function as a Lewis acid to assist the C_4-OH bond cleavage, which triggers the dehydroxylation of the HMBPP and generates an allyl radical-$[4Fe\text{-}4S]^{2+}$-H_2O intermediate. These two proposed intermediates are specific for the Birch reduction. With the second one-electron reduction (from an outside source), the protonation products IPP and DMAPP would form. Alternatively, the allyl radical-$[4Fe\text{-}4S]^{2+}$-H_2O intermediate first obtains the proton, generating a product-$[4Fe\text{-}4S]^{3+}$-H_2O intermediate, which is similar to an intermediate proposed in the bio-organometallic model (which is described in the following section).

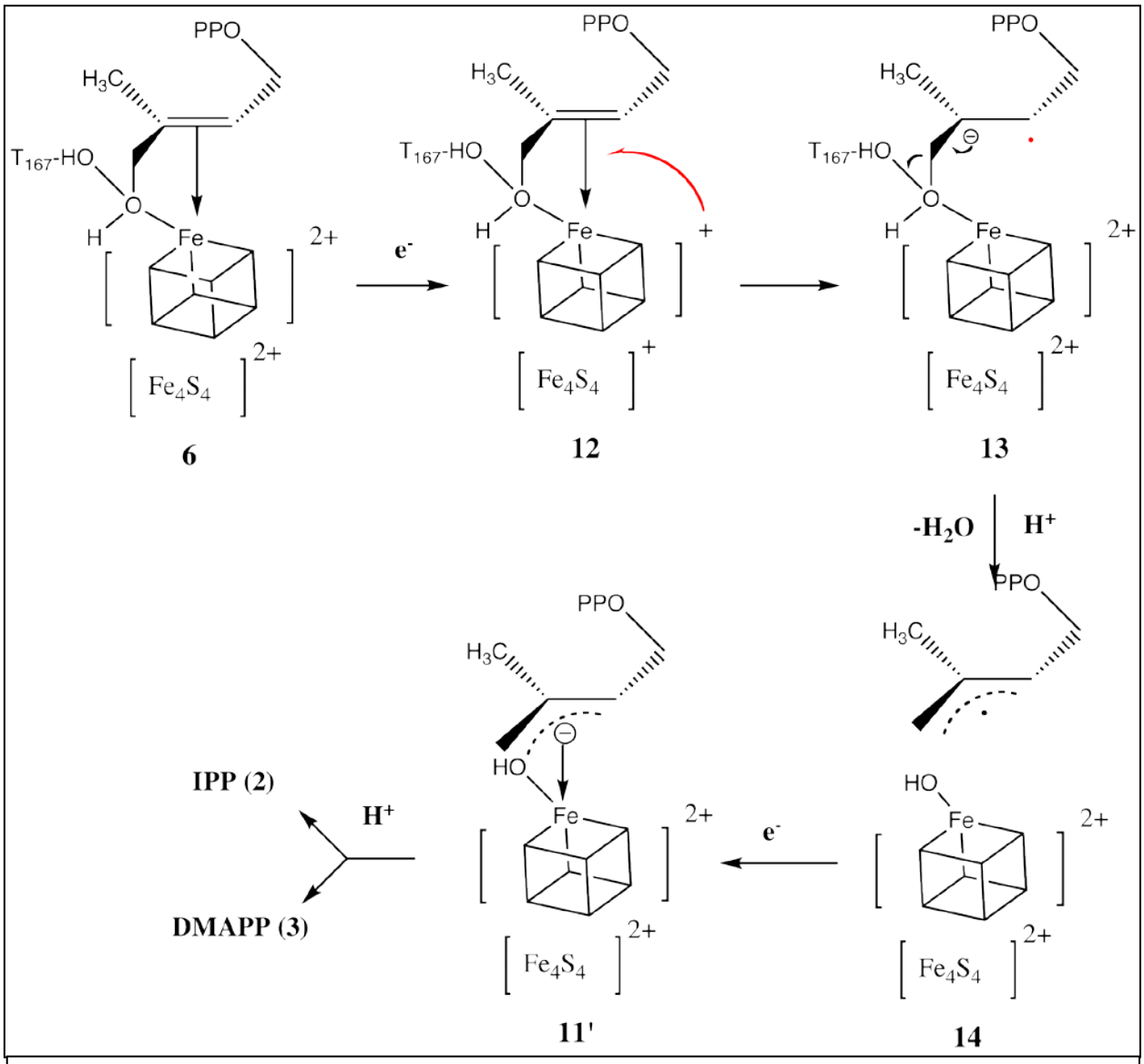

Figure 1-16 Birch reduction model (see text for more details)

This proposal is supported by biochemical analog studies. A series of substrate analogs (Figure 1-17) were prepared to study the interactions in the active site during IspH catalysis and to gain insight into the catalytic mechanism of IspH. The first is the [4-F]-analog, which carries a fluoro instead of hydroxyl group at the C_4 position. Since fluoro is a poor metal ligand, this analog produced IPP and DMAPP at a ratio of 7:1, with a ~115-fold reduction in k_{cat}/K_M. Another

analog has the fluorine at C_5 instead of C_4, this analog not only reduced the direct coordination between analog and the cluster, but also changed the water network (T163 and E126) conformation at the active site, which resulted in a dramatically ~1783-fold reduction in k_{cat}/K_M, and IPP was the sole product from this analog. These two results confirmed that the coordination of C_4-OH of the substrate HMBPP to the unique iron site of the [4Fe-4S] cluster is crucial for effective IspH catalysis. But this is inconsistent with the bio-organometallic model.

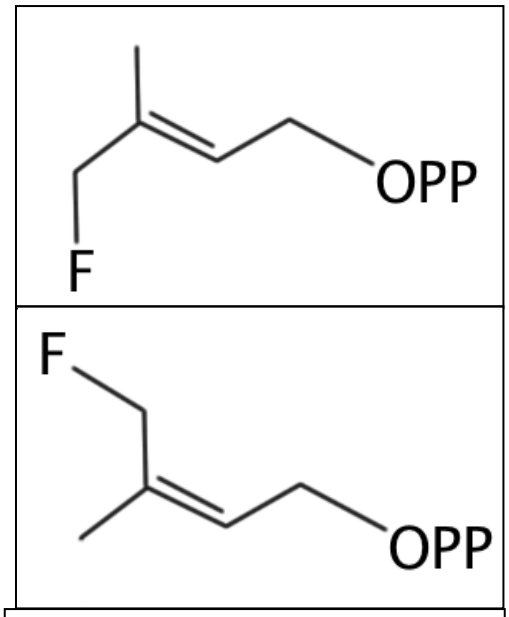

Figure 1-17 Substrate analogs

1.4.2. Bio-organometallic model

Based on the EPR and crystallography studies on both wild type and mutant IspH, the bio-organometallic model was propose by the Oldfield group (Figure 1-18) (28, 29). The reaction begins with binding of IspH to HMBPP through the C_4-OH. The close proximity of the double bond of HMBPP to the unique iron results in the formation of a π complex or η^2-alkenyl/metallacycle intermediate (Figure 1-18, intermediate II). This is accompanied by the rotation of the C_4-OH group to the other site where it interacts with E126, and with its own pyrophosphate group via a β-phosphate H-bond. (This evidence is still questioned, since the rotation was observed only in the inactive E126Q mutant.) This is then followed by a two-electron reduction, very much like ferredoxin:thioredoxin reductase, resulting in the

dehydroxylation and formation of a highly oxidized high potential iron-sulfur protein (HiPIP) like an η^1-allyl $[4Fe\text{-}4S]^{3+}$ intermediate, or an allyl anion-$[4Fe\text{-}4S]^{3+}$ intermediate (Figure 1-18, intermediate III). Subsequent reduction and protonation yields the product IPP and DMAPP.

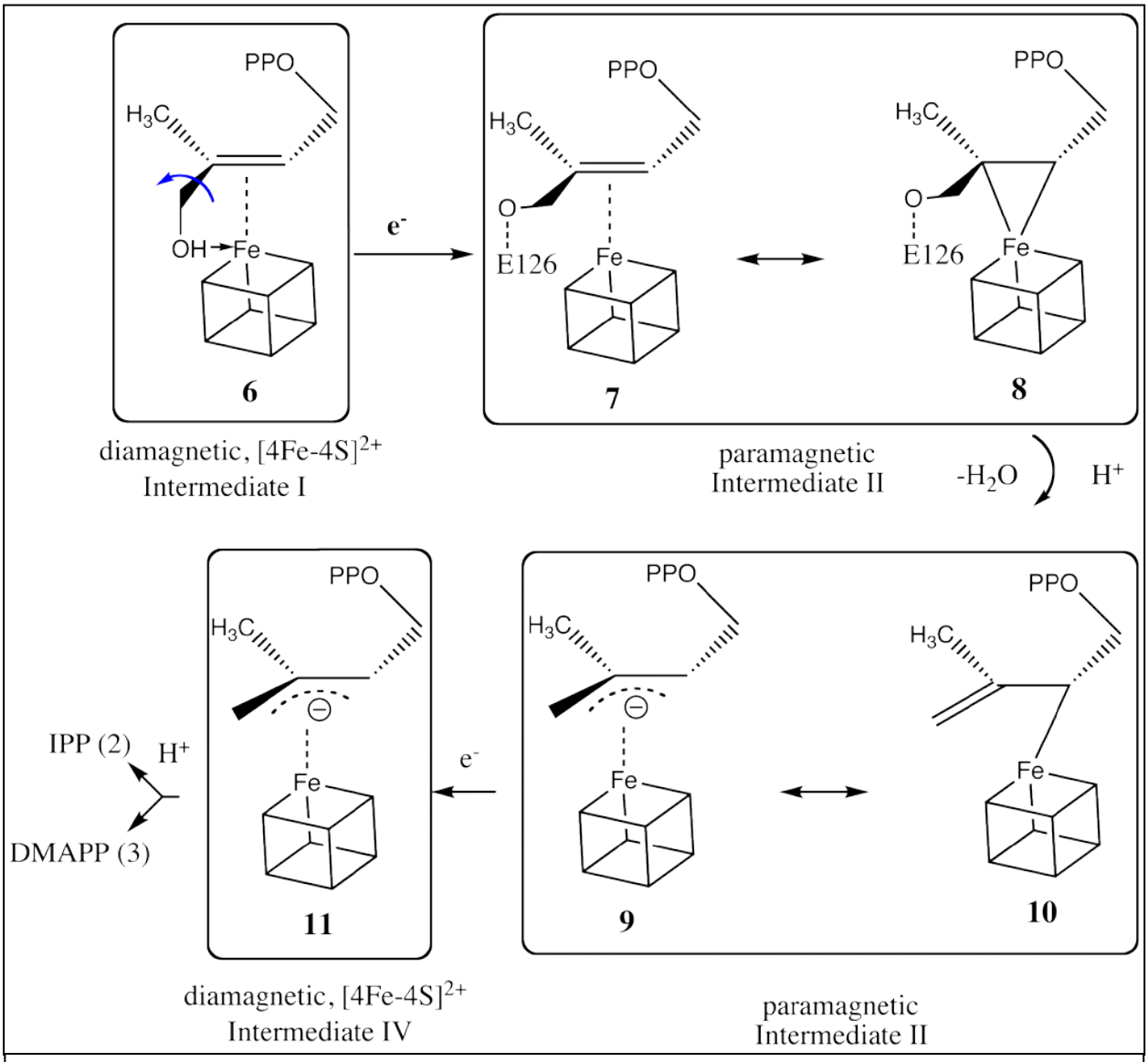

Figure 1-18 Bio-organometallic model

The bond rotation in this hypothesis is unique. As mentioned earlier, this “intermediate II” was successfully trapped by EPR/ENDOR and crystallography studies while incubating IspH E126A or E126Q mutants with dithionite and substrate HMBPP. The intermediate is a paramagnetic

species with g-values of 2.124, 1.999. 1.958. (Figure 1-19). HYSCORE studies show very weak ^{17}O hyperfine interaction indicating that in this state there is no direct bond between the cluster in the E126Q mutant and the C_4-^{17}O of the substrate. This was, consistent with the structure reported from a crystallography study of the intermediate IspH/E126Q- HMBPP complex.

The catalytic relevance of this species, however, is questioned since the E126 mutant is inactive. The "intermediate III" is assigned to a species that is detected in freeze-quench studies, following incubation of 30 equivalents of dithionite and 10 equivalents of substrate with wild type IspH for 10 seconds. This paramagnetic species has g-values of 2.171, 2.010, 1.994, and this is also observed in so-called one-electron reduced experiments (which are been described in the next chapter) where this is a stable species due to lack of electrons to complete the reaction cycle. This species was dubbed FeS_I by our group.

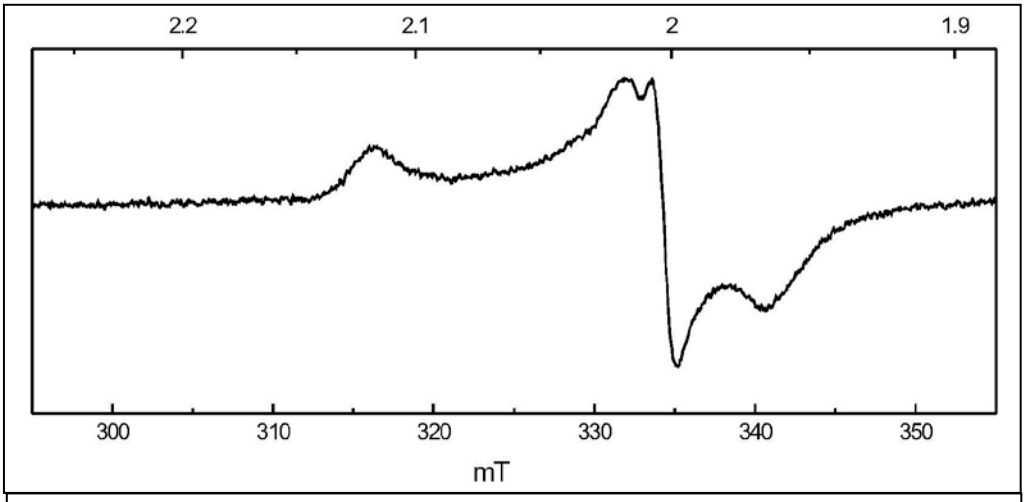

Figure 1-19 Proposed reaction intermediate observed in mutant E126Q IspH. The paramagnetic species has g-values of 2.124, 1.999, and 1.958.

1.4.3. Highlighting previous results obtained in the Duin laboratory.

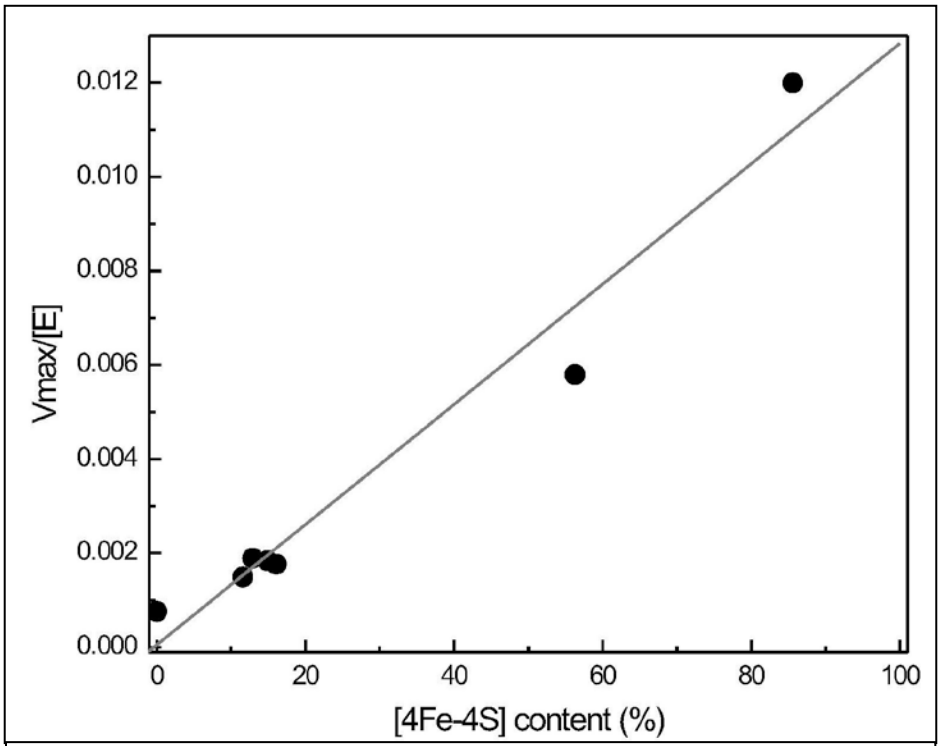

Figure 1-20 A linear relationship between the enzyme activity and cluster content was discovered

In our lab, Dr. Weiya Xu made 3 major discoveries with IspH. First, she discovered the linear dependency of enzyme activity on [4Fe-4S] content in *P. falciparum* IspH. This was done by performing iron determinations in combination with kinetic studies for three different types of enzyme preparations: as-isolated enzyme (±15% cluster content), reconstituted (60-86% cluster content), and exposed to air for a prolonged period of time (0% cluster content). A linear relationship was discovered (Figure 1-20). This work was relevant because at that time it was proposed by several groups that the [3Fe-4S] cluster forms of the enzyme were the active forms and not the [4Fe- 4S] form.

Second, she made a form of the enzyme where first the cluster was reduced with dithionite which was subsequently removed by running the enzyme over a desalting column. By incubating this one-electron-reduced enzyme (from *Aquifex aeolicus*, *Plasmodium falciparum* and *E .coli*) with substrate, a paramagnetic signal, FeS_I with g-value of 2.173, 2.013, and 1.997, was observed in

EPR spectroscopy (Figure 1-21). This is a stable species. Besides, it is not a dead-end product, because when additional dithionite was added to this species the FeS_I signal vanished, presumable completing the reaction cycle. She did not show however, whether IPP and DMAPP were generated after the FeS_I disappeared. In addition, the catalytic competency is not clear since it develops on a time scale of seconds to tens of minutes with is longer than the k_{cat} observed in kinetic studies. These studies, however, used a more powerful reductant, methyl viologen instead of dithionite.

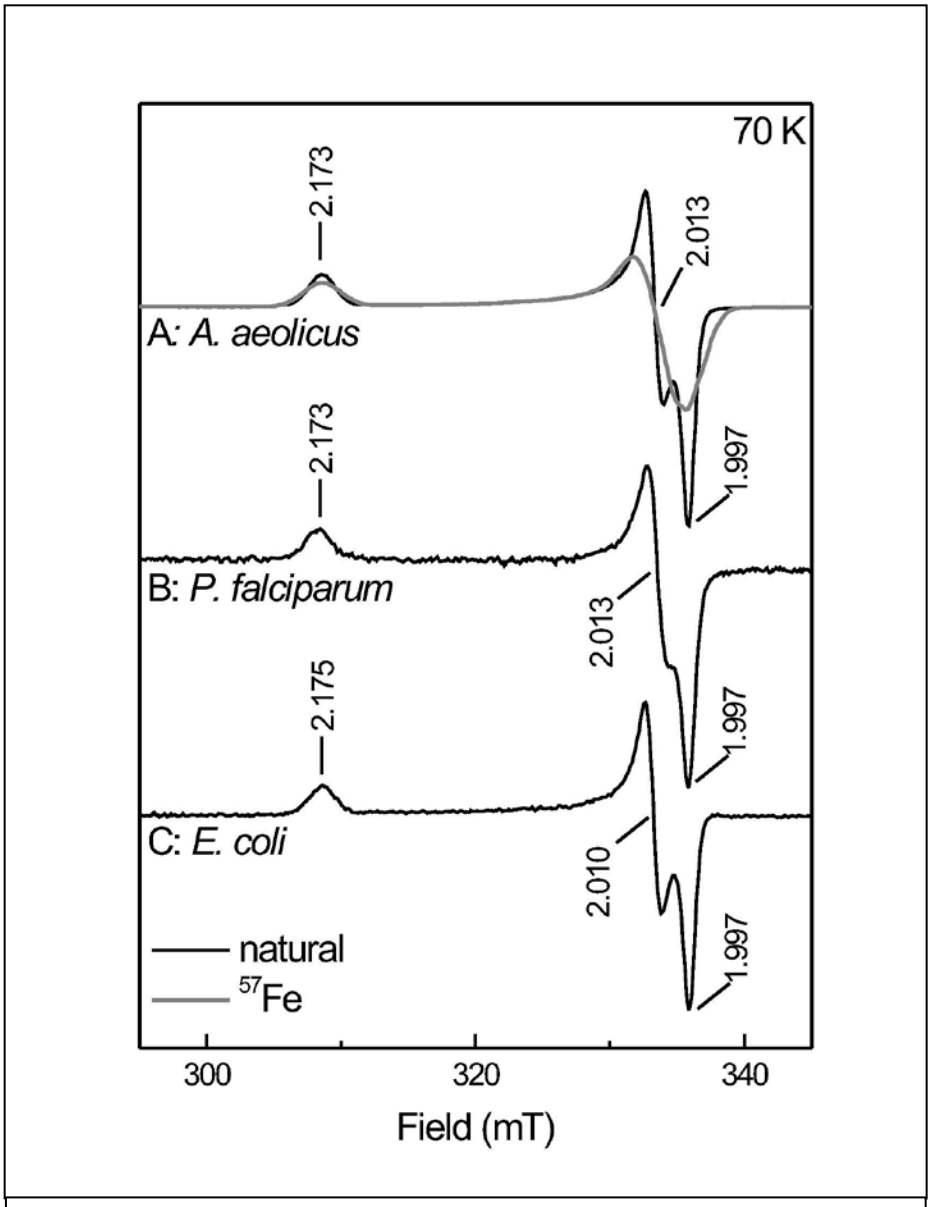

Figure 1-21 FeS_I species detected in three different IspH enzymes

Third, she characterized the roles of 3 important residues: H42, H124 and E126 from *A aeolicus*. Since the histidines were proposed to bind the pyrophosphate group of the substrate HMBPP, and glutamate was predicted to play an important in the actual reaction mechanism. Two mutants were made for each residue: H42A, H42F, H124A, H124F, E126A, E126Q. All of them have the cluster contents in the range of 10-20%, which could be improved by reconstitution to 40-50%. Experiments like kinetic studies (Table 1-2), and EPR measurement (Figure 1-22) were performed with each mutant.

Reconstituted enzyme	Cluster content (%)	Specific activity after correction for cluster content (µmol min^{-1} mg^{-1})	K_M (µM)	k_{cat}/K_M
WT	42.9	1.95	6.4	0.3
H42A	29.9	0.2	1.7	0.12
H42F	45.9	1.09	144	0.008
H124A	33.2	0.4	1.2	0.1
H124F	35.6	0.2	33.6	0.006
E126A	41	0.19	2.4	0.08
E126Q	29.6	0.2	0.4	0.5

Table 1-2 Kinetic study result

(1) H42 mutants: The kinetic data showed that only the H42F mutant still possess 50% activity in comparison to wild-type enzyme. The EPR spectrum of H42A (Figure 1-23 A), obtained by mixing the HMBPP with reconstituted and one-electron reduced enzyme and subsequent freezing after 30 second of incubation, showed only the $[4Fe\text{-}4S]^{1+}$ signal at 10K and very little FeS_I signal at 50K. As for H24F, the EPR spectrum (Figure 1-23 B) showed the $[4Fe\text{-}4S]^{1+}$ signal at 10K and a mixture of both the $[4Fe\text{-}4S]^{1+}$ and FeS_I signals at 50K, which together with the kinetic result showed that this mutant can still perform the full reaction albeit much slower and a much higher K_M value. It was concluded that His24 is important for binding the substrate.

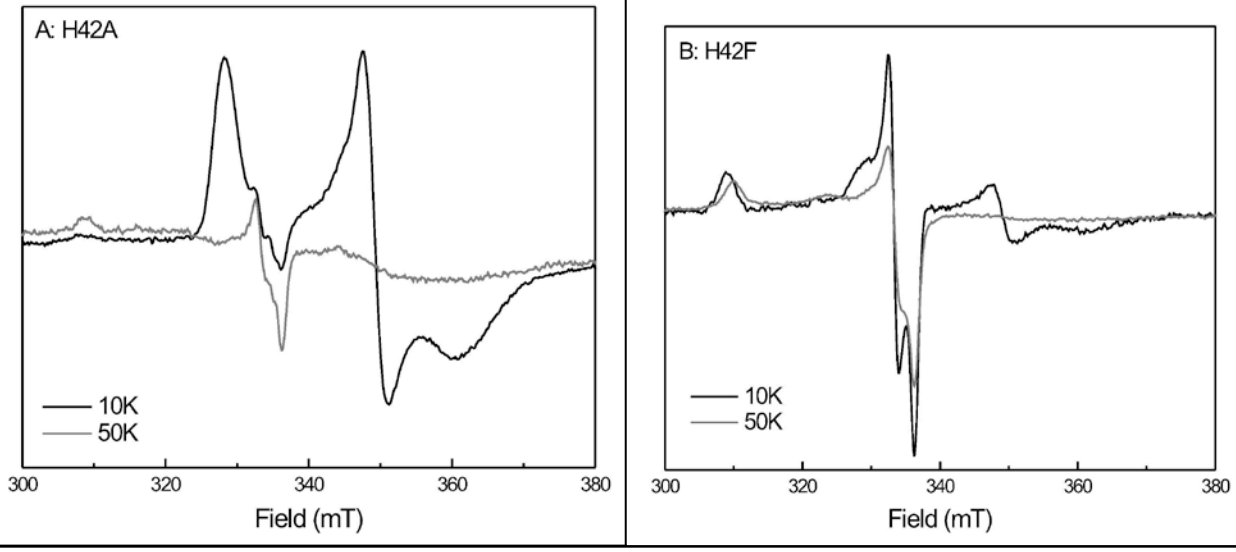

Figure 1-23 EPR spectra for H42 mutants

(2) H124 mutants: This residue was first predicted to have the same function as H42 as a substrate binding residue. But neither of the two mutants of H124 showed significant activity. EPR studies showed that the substrate caused the loss $[4Fe\text{-}4S]^{1+}$ signal, probably via a direct oxidation (Figure 1-23 C, D). In both cases small quantities (less than 5%) of the FeS_I species

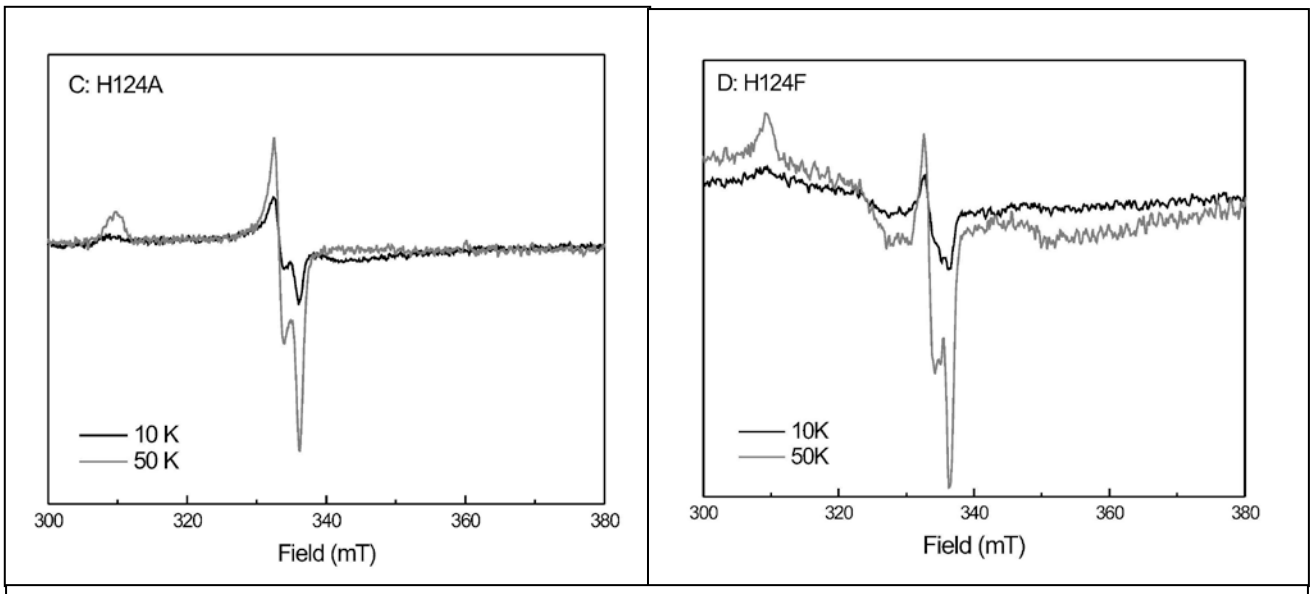

Figure 1-23 EPR spectra for H124 mutants

were detected and in some samples a radical-like signal was detected (not shown). Based on this data it was proposed that His124 might play a role in the correct orientation of the substrate in the active site. If the substrate is not orientated properly substrate-based radical are formed instead of the FeS_I species.

(3) E126 mutants: It was proposed that E126 either binds to HMBPP at the C_4-OH directly or through a water molecule and that E126 or the water molecule play a role in the direct protonation of a reaction intermediate. The complete loss of activity appears to be in line with this proposal. The EPR data show that same species as earlier described by the Oldfield group with g_{123} = 2.120, 2.002, 1.965. In contrast to the FeS_I signal when excess dithionite was added to the enzyme/substrate mixture, this signal does not become a transient signal but develops rapidly after which it stays stable for a long time period. This indicates that it is a dead-end product. It could be another intermediate of the mechanism as propose by the bio-organometallic hypothesis, or, it can also be totally irrelevant to the actual catalytic reaction.

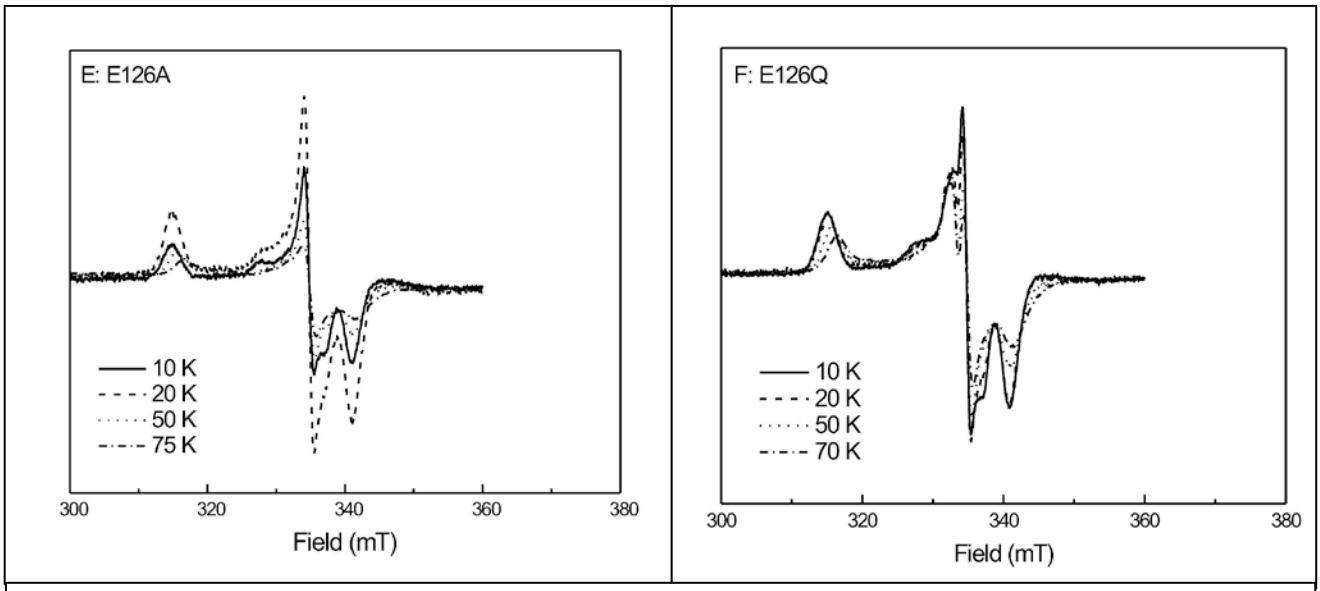

Figure 1-23 EPR spectra for E126 mutants

1.5. Challenges we are facing

First, since the activity of the enzyme is linearly dependent on the cluster content, the most important objective is to improve the cluster content. Because we are also planning to do Mössbauer studies with this enzyme, we want to avoid the cluster reconstitution procedures that normally introduce iron species that are very difficult to remove from the protein sample. Instead, we opted for the natural occurring cluster synthesis.

Second, the earlier experimental results were obtained with one-electron reduced enzyme. It is not completely clear if the FeS_I species is a true reaction intermediate. It is important to show that this species can be detected under both pre- and steady-state conditions. Using the rapid-freeze/quench method, incubating the enzyme with substrate and excess electron donor (dithionite) for different time periods, a serial set of EPR spectra can be obtained that would put these species in the context of the whole reaction.

Third, when the FeS_I species it is shown to be a true reaction intermediate, it will be important to prove what type of intermediate it is. Most importantly, the oxidation state of the cluster has to be determined. With the Mössbauer spectroscopy technique, we can examine the iron charge of each iron in the intermediate.

Fourth, earlier experiments for characterizing the roles of the important residues such as histidine, cysteine, and glutamate, were carried out with *A. aeolicus* enzyme. We want to repeat that work with the *E. coli* enzyme. In addition, the Tyr167 mutant has not been studied yet. This

residue is reported to participate in the active site water/H-bond network and is most likely the direct donor of protons to HMBPP.

Chapter 2: Materials and Methods

2.1. Chemicals

First of all, the substrate HMBPP was synthesized by Selamawit Ghebreamlak under the instruction of Dr. Forrest Smith at the Department of Pharmacal Sciences, Auburn University, following the a procedure from the literature (30, 31). Methyl viologen dichloride hydrate 98% was purchased from Sigma ALDRICH, and Sodium Hydrosulfide, tech., 85+% Powder (Dithionite) was purchased from Alfa Aesar. Imidazole was purchased from Fisher. The 5 mL Ni-affinity column for protein purification was purchased from GE healthcare life sciences.

2.2. Plasmids

Earlier research showed that the activity of IspH is linearly dependent on the Fe-S cluster content. Therefore it is essential to produce protein samples with close to 100% cluster content. This can be done by using cluster reconstitution methods with the apo-enzyme. This, however, also produces iron species that will be detectable in Mössbauer spectroscopy. Therefore we will try to increase the cluster content using a genetic approach and co-express specific cluster insertion proteins. To establish the success of this method, the cluster content of enzyme expressed under three different conditions needs to be compared: 1) expressed by itself, 2) co-

expressed with the ISC enzymes, 3) co-expressed with the ErpA enzyme. (Co-expression with both the ISC genes and the *erpA* gene is planned for the near future.) These experiments were carried out for IspH from *Aquifex aeolicus*, *Plasmodium falciparum*, and *Escherichia coli*, which resulted in 9 different protein preparations.

The *ispH* genes from *Aquifex aeolicus* and *Plasmodium falciparum* were amplified by PCR and ligated into the pQ60 plasmid/vector. The plasmids encode ampicillin resistance. The genes were expressed under anhydrotetracycline. These plasmids were provided by the group of Dr. Hassam Jomaa at the Justus-Leibig University at Giessen, Germany.

The IspH H124F and E126Q mutants from *Aquifex aeolicus* were encoded on the pASK-IBA3^{+} plasmid. The plasmid encodes ampicillin resistance. The gene is expressed under anhydrotetracycline. These plasmids were donated by the group of Dr. Oldfield at the University of Illinois, Urbana-Champaign, IL.

The *ispH* gene was amplified from *Escherichia coli* K12 genomic DNA by PCR and then ligated into the pQE30 plasmid. The plasmid encodes ampicillin resistance. The gene is expressed under anhydrotetracycline. This plasmid was donated by Dr. Michael Groll at the Center of Integrated Protein Science at Munich, Germany.

The *isc* genes were ligated into the pDB1818 plasmid. The plasmid encodes kanamycin resistance, and the genes are expressed under arabinose induction. This plasmid was constructed

by Dr. Biswarup Mukhopadhyay at the Virginia Bioinformatic Institute at Virginia Tech, and donated by Dr. Dennis Dean.

Finally, the *erpA* gene was amplified into a pUC18-derived plasmid. This plasmid encodes kanamycin resistance and the gene was expressed under arabinose. The plasmid was donated by the group of Dr. Frédéric Barras at the Department of Chemistry bacterial, National Centre for Scientific Research, France.

2.3. Cell Strain Construction

(a) 100 µL *E. coli* XL-1 Blue Competent Cells (Stratagene) were obtained from the -80°C freezer and kept on ice in a 14-mL BD Falcon polypropylene round-bottom tube. 20 µL of one of the plasmids was added and the suspension was incubated for 30 minutes. A heat shock was applied at 42°C for 45 seconds, followed by incubation on ice for 2 minutes. 0.9 mL antibiotic-free SOC medium was added and the solution which was subsequently incubated in a shaker at 37°C for 1 hour with a speed of 225-250 rpm. The cell culture was transferred into a micro-centrifuge cup and centrifuged at the speed of 14,000 rpm for 5 minutes. The supernatant was discarded and another 0.1 mL SOC medium was added to the cell pellets. The redissolved cells were plated on LB agar plates that contained ampicillin. The plates were incubated at 37°C for 12-16 hours. Plates that showed colonies were stored at 4°C. Cells have to be replated every month.

(b) To construct a strain that contains two plasmids, cells that already contained the other plasmid were used as the host cells. These were treated with calcium chloride to make them

competent again. First, the cells with the ^{Amp}IspH plasmids were grown in 5 mL ampicillin-containing SOC medium in a 25mL flask. The culture was incubated overnight at 37°C under shaking (225-250 rpm). The cells were transferred to 50 mL SOC medium with ampicillin in a 250 mL flask. When the OD at 600 nm reached 0.25-0.3, the cell culture was cooled for 15 min on ice followed by a centrifugation step at 186×g for 10 min (Beckman XL-70 Ultracentrifuge, YPE 45 Ti Rotor, Beckman Coulter, Inc.). The supernatant was discarded and the cell pellet resuspended in 40 mL cold 0.1 M $CaCl_2$, followed by incubation on ice for 30 minutes. This was followed by another centrifugation step at 186×g for 10 min. The supernatant was discarded and the cell pellet was resuspended in 6 mL 0.1 M $CaCl_2$ with 15% Glycerol. The final solution was pipetted into sterile micro centrifuge cups, 0.4-0.5 mL per tube, and stored at -80°C until use.

The transformation step is similar with the protocol described as above. First cells containing ^{Amp}IspH were treated with calcium chloride to become competent. The second plasmid (isc or ErpA) with kanamycin antibiotic resistance was added and the regular protocol was followed. After constructing the cells, new plates containing both ampicillin and kanamycin were used. Only the cells that contain both plasmids should form colonies.

2.4. Cell Growth

Strains that overexpress the *ispH* genes were grown in SOC medium (1 L contains 20 g tryptone, 5 g yeast extract, 0.5 g NaCl, 10 mL 1M $MgSO_4$, 10 mL 1M $MgCl_2$, and 20% glucose). Strain that co- or overexpress the *erpA* genes were grown in LB medium (1 L contains 10 g NaCl, 10 g Bacto-tryptone. 1 M $FeCl_3$ was added to all cultures. Cells that contained the *ispH* gene needed 100 mg of ampicillin as antibiotic and 0.1 mg anhydrotetracycline as inducer per liter. Cells that contained *isc* or *erpA* gene needed an additional 50 mg of kanamycin as antibiotic and 3 grams of arabinose as inducer per liter.

One colony from the LB plate was inoculated in 5 mL of SOC/LB medium which contained the appropriate antibiotics. The culture was kept at 37°C for at least 6 hours under shaking (225-250 rpm). The culture was transferred to 100 mL SOC/LB medium plus of 30 μL of 1 M $FeCl_3$, and was incubated overnight under shaking. The cell culture was transferred the next morning to 1-4 L SOC/LB medium with an additional 300 μL 1 M $FeCl_3$ per liter. After another 3 hours of shaking, the O.D. of the cells at 600 nm would reach 0.4-0.6, and the inducers, anhydrotetracycline, arabinose, and/ or lactose were added. When the O.D. of the cells at 600 nm reached 3, the cells were harvested by centrifugation (BECKMAN J2-MI centrifuge at 4424×g for 20 minutes). The supernatant was decanted and cell pellets were stored at -80°C.

2.5. Protein purification

Since IspH is oxygen sensitive, the purification was performed in the Coy tent (Figure 2-1) with an atmosphere of 95% Nitrogen and 5% Hydrogen. Oxygen that leaks in is continuously removed by a palladium catalyst and is kept in the 0-5 ppm range. All the buffers were filtered and subsequently boiled to get rid of dissolved gasses. The solutions were cooled down under a vacuum in stoppered bottles for at least 2 hour. After this the bottles where pressurized with Ar to 0.5 Atm after which the bottles could be stored for several months. Buffer A contains 30 mM Tris-HCl (pH 8.0), and 100 mM NaCl. Buffer B contains 30 mM TrisHCl (pH 8.0), 100 mM NaCl, and 500 mM imidazole. All plastic materials were incubated overnight in the Coy tent to remove any oxygen that sticks to the surface.

Figure 2-1 The anaerobic tent

The cell pellet from 1 L culture (fresh or from the -80 °C freezer) was resuspended in 100 mL buffer A. The cell membrane was broken using ultrasound (BRANSON Sonifier 450 Digital Ultrasonic Homogenizer) by pulsing for 7 min (0.5 sec intervals). This was repeated several times dependent on the color of the suspension. The crude extract was centrifugated (Beckman XL-70 Ultracentrifuge, 45Ti Rotor, Beckman Coulter, Inc.) at 7266×g for 30 minutes. The enzyme is in the supernatant. The enzyme from *A. aeolicus* is a heat stable enzyme and two additional steps were included, the cell extract solution was incubated at 65°C for 30 minutes, followed by another step of centrifugation. The cell extract was filtered using a 0.45 μM Millipore filter, and loaded on to a pre-washed His-trap Ni^{2+} affinity column. After the loading step, the protein was eluted by the increasing amount of imidazole (buffer B). This procedure was done at an AKTA FPLC (GE HeadCase). IspH from *A. aeolicus* and *P. falciparum* was eluted with an imidazole concentration around 225 mM, and IspH from *E. coli* was eluted with an imidazole concentration around 75 mM. The protein was collected and used freshly.

2.6. UV-absorption

Several properties of IspH can be measured by absorption spectroscopy measurements. The concentration can be determined by the absorbance at 280nm due to the tyrosine and tryptophan content ($\varepsilon = 26930\ M^{-1}cm^{-1}$). The presence of single iron ions is detectable as a peak at around 310nm. The single iron ion content can be reduced by running the protein sample through a desalting (PD10) column.

2.7. Iron determination

All material (e.g. tubes, pipette tips) for this step needed to be pre autoclaved, and washed in 1M HCl to remove bound iron ions. A set of iron standards (0, 10, 20, 30, 40, and 50 μM) was prepared by dissolving ferrous ethylenediammonium sulfate in 0.01 M HCl. Two reagents are needed for the determination: Reagent A, also called iron releasing agent, is composed of equal amounts of 4.5% $KMnO_4$ and 1.2 M HCl, and has to be prepared freshly. Reagent B, the iron chelating and releasing agent, contains 9.7 g ammonium acetate, 8.8 g ascorbic acid, 80 mg ferrozine, and 80 mg neocuprione in 25 mL distilled water. This reagent can be stored on the shelf for a month.

1 ml protein samples were prepared with different concentrations (e.g. 5x, 10x, 20x, and 40x dilution). 1 mL samples of the iron standard underwent the same procedure. 0.5 mL reagent A was added to each sample, which were subsequently incubated at 60°C for 2 hours. This was followed by the addition of 0.1 mL reagent B and incubation at room temperature for half an hour. The absorption at 562 nm was measured for each sample. The results for the standard were plotted in origin and should show a linear relationship between the absorption and the iron concentration. Using the calibration curve the unknown Fe concentration of the protein samples was calculated. Since every cluster contains 4 iron ions, the iron concentration needs to be divided by 4 to get the cluster content.

2.8. SDS-Page

Sodium dodecylsulfate polyacrylamide gel electrophoresis (SDS-PAGE) is the most common type of denaturing electrophoresis. The gel was prepared in the crevice between two glass plates. A plastic comb was applied to the crevice to generate the wells. The gel could be used directly or wrapped with wet towels and stored in the 4°C refrigerator.

Buffers need to be prepared: (a) Sample buffer: 1.5 mL of 1 M Tris-HCl pH 6.8, 3 mL of 1 M dithiothreitol, 0.6 g sodium dodecyl sulfate), 0.03 g bromophenol blue, and 2.4 mL glycerol - final volume 7.5 mL. (b) 10X concentrated Running buffer: 248 mM Tris (30 g), 1.92 M glycine (144 g), and 1% w/v sodium dodecyl sulfate (10 g) per liter. (c) Coomassie staining solution: 1.25 g Coomassie, 225 mL methanol, 225 mL H_2O, and 50 mL glacial acetic acid per liter. (d) Destaining solution: 300 mL methanol, 100 mL acetic acid, and 600 mL H_2O per liter.

The SDS-PAGE apparatus was assembled and running buffer was added. 10 µL of protein solution was mixed with 10 µL sample buffer, heated at 95°C for 5 minutes, and centrifuged for 3 minutes at 14,000 rpm in an Eppendorf centrifuge. 5 µL of the supernant was applied into wells present in the stacking gel. The same procedure was done with 5 µL of protein marker. The gel was run at a power of 130 V for 45 minutes. The gels were incubated in the coomassie staining solution for 15 minutes, subsequently rinsed with water, and incubated overnight under mild shaking in the destaining solution. The complete gels were scanned and some of them stored in water.

2.9. Kinetic studies

To obtain the kinetic parameters for the conversion of HMBPP by IspH a colorimetric method was used. The direct electron donor was reduced methyl viologen which is also the colored indicator for the assay. Methyl viologen was reduced by a half equivalence of dithionite. The assays were conducted using an UV-visible spectrophotometer. The oxidation of the dithionite-reduced methyl viologen was followed at 603 nm (ε_{603} is 13,600 $M^{-1}cm^{-1}$). In the quartz cuvette, each 1 mL of sample contained 50 μM dithionite, 100 μM methyl viologen, 5 μM IspH, and the substrate HMBPP ranging from 4 to 300 μM.

Figure 2-2 The anaerobic box

The whole experiment was carried out in an anaerobic box to prevent any interference from oxygen (Figure 2-2). All components were added to a cuvette, except the substrate HMBPP, and incubated at 25°C for 30 seconds. The control is the baseline shift under these conditions. The reaction was started with the addition of substrate. Every point was repeated 3 times. The Origin program (from OriginLab Corporation) was used to make Michaelis-Menten plots and fitting of the curves.

2.10. Freeze quench

Freeze quench is a method that uses an extremely cold environment to stop/quench a reaction. This is a relatively safe and straight forward method which does not introduce any unnecessary chemicals to the protein solution. With the reaction quenched at a series of different time points, the formation of intermediates or products according to the time can be observed with EPR spectroscopy when these compounds are paramagnetic.

Figure 2-3 Kin-Tek freeze-quench machine

A KinTek Quench Flow machine was used for the short reaction times (Figure 2-3). The machine contains two parts: the stop flow machine itself and the packing station. The protein (in

our case premixed with dithionite) and the substrate solution were both loaded into separate drive syringes. The protein concentration needs to be at least 400 μM to provide enough signal after mixing. The syringes were emptied simultaneously. The solutions were mixed in a mixing chamber followed by a run through an aging tube. The speed of the flow and the selection of the aging tube were all done electronically after the desired reaction time (4.6 ms, 20 ms, 50 ms, 100 ms, 500 ms, 1 s, etc.) was entered on the electronic control pad. The aging tube ends in a nozzle from which the mixed solution is sprayed into cold isopentane (-140°C) which caused an immediate freezing of the sample, quenching, which stopped the reaction (Figure 2-4). The sample comes out as a fine 'snow' and has to be kept cold while attempts are being made to collect most of the snow by packing it at the bottom of an EPR tube. Due to empty spaces between the solution particles about 30% signal intensity is lost.

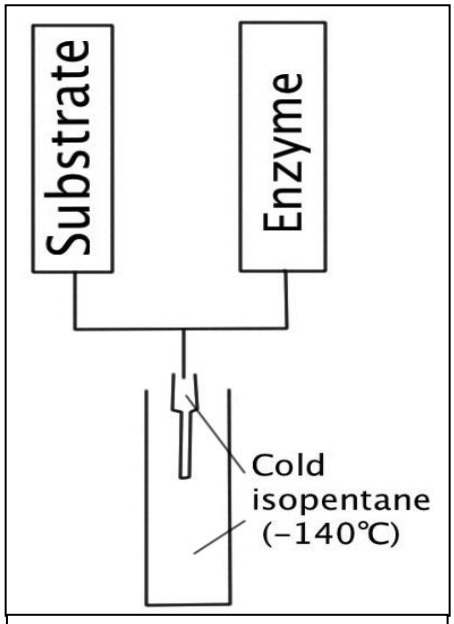

Figure 2-4 Schematic setup of the freeze-quench experiment (see text for details).

Samples for longer reaction time points can be prepared by mixing the protein (containing 66 mM dithionite) and substrate by hand, followed by the prerequisite incubation time (5 s, 10 s, 20 s, 40 s, 1 min, 3 min, 5 min, 10 min, etc.), and quenching in cold ethanol (-114°C).

Here we studied *A. aeolicus* wild type IspH and two of its mutant, E126 and H124F, and *E. coli* wild type IspH. Several different types of experiments were carried out: (a) One-electron reduced experiment. The electron donor dithionite was added to the protein, followed by and incubation

step for 15 minutes. The excess dithionite was removed by running the sample over a desalting (PD10) column. With this treatment, the cluster is still reduced and can provide one electron to the reaction. Since there is no additional dithionite present the reaction should stall at this point. We call this the one-electron-reduced form of the protein. We expect to see with the addition of substrate the formation of a reaction intermediate but no product. (b) Steady State Reaction. Excess dithionite was added to the protein. The solution was mixed against 10 equivalent of substrate. The intermediate should form and disappear. Then a product (signal) could form and stay. (c) Single-turn-over Reaction. The excess dithionite was added to the protein and the solution was mixed with only 1 equivalent of substrate. The same signals as under 'b' should be observed albeit with much lower intensity but a turn-over number could be deduced from the data set.

2.11. EPR measurement

The main detection technique used in our laboratory is electron paramagnetic resonance (EPR) spectroscopy, also called electron spin resonance (ESR) spectroscopy. Since this is not a 'standard' technique a small introduction will be presented here.

2.11.1. Brief introduction

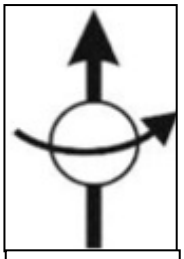

Figure 2-5 A free unpaired electron in space

EPR spectroscopy is a technique based on the absorption of electromagnetic radiation by a paramagnetic sample placed in a magnetic field. The absorption of a sample is dependent on its own character and reacts according to the

frequencies and magnetic field which are applied to it. In 1944, the first EPR experiment was done by E.K. Zavoisky (32, 33). Seven decades later, EPR now has a broad range of applications in the field of physics, chemistry, biology, earth science, and material science.

A free unpaired electron in space, always has an intrinsic angular momentum, called "spin', S, and will generates a magnetic field, μ (magnetic momentum) (Figure 2-5). By adding an outside magnetic field B_0, such as a magnet in the laboratory, unpaired electrons in the samples will show the Zeeman Effect (Figure 2-6). For an electron $\mu = g_e \beta m_s$, and the electronic Zeeman energy is: $E = -\mu B_0$, where g_e is the g-factor of the free electron and equals 2.0023192778 (≈2.00). β is the Bohr magneton. The value of m_s depends on the electron's direction. It has a value of -1/2 while the electron is parallel the B_0 field, and +1/2 while its anti-parallel to B_0.The electron can change orientation by absorbing electromagnetic radiation which exactly equals the state energy difference: $\Delta E = h\gamma$, where h is the Plank's constant, and γ is the frequency of the radiation. When the net population difference is big enough, the resonance condition

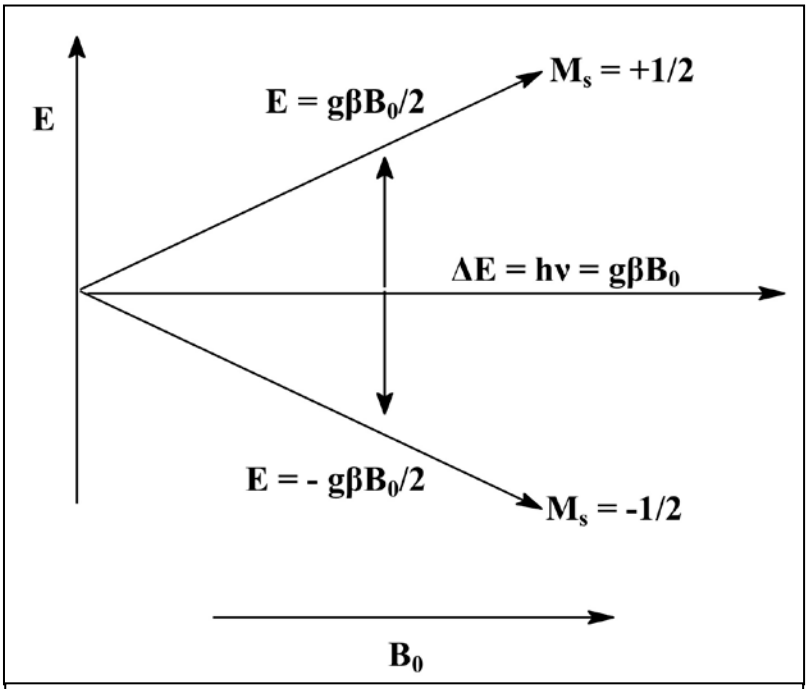

Figure 2-6 By adding an outside magnetic field B_0, such as magnet in the laboratory, unpaired electrons in the samples will show Zeeman effect.

is achieved and radiation is absorbed and an EPR signal can be detected. Under these conditions: $\Delta E = g_e \beta B_0 = h\gamma$.

By placing the electron on to a nucleus, besides its own S, it will also generate an orbital angular momentum (L), now $\mu \propto g_e S+L$ ($\propto$ means proportional to). And L will generate a spin-orbital coupling, which is actually proportional to S. Since L is unknown we switch to using g instead of g_e to represent how the electron is affected. Now the value of g will different from g_e and has becomes a characteristic property of the paramagnetic species. We also adapt ΔE to $\Delta E = g\beta B_0$. The value of g is determined by the size and shape of the nucleus. That is why electrons associated with H, O, C, and N atoms always have a g-value close to g_e, while transition metals have significantly different g-values.

We can obtain the g-value by using a microwave source with a set frequency and wavelength to irradiate the sample and sweep the magnetic field. When the resonance conditions are satisfied absorption will occur. The value of g can then be calculated by:
$g = h\gamma/\beta B_0 = 0.714484\ \gamma$ (MHz) / B_0 (Gauss) for the X-band frequency of 9.4 GHz.

The g-value is angular dependent and reflects the electronic 3D environment experienced by the electron. Biological EPR samples are prepared by freezing a protein solution and all possible molecule orientations are present (powder sample). By placing the paramagnetic sample, with a xyz axes system, into an external dipolar magnetic field B with a field vector B along the z-axis, imagine the xy plane of the molecule is parallel to the magnetic field, and its z-axis is perpendicular to it. During the EPR measurement, the outside magnitudes change as the field is

rotated in order to swipe the electronic 3D environment structure of the molecule. When the vector of the magnetic field changes from z to y, the resonance B in equation $g\beta B = h\gamma$, will smoothly changes between two extreme from B_z to B_y. On the other hand, when the vector of the magnetic field changes from y to x, the change of the EPR absorption line will be relatively small and even zero when $g_y = g_x$. The EPR spectrum is dependent on the 3D structure of the paramagnetic metal center. While the sample is isotropic, $g_x = g_y = g_z$, since the energy slowly change between two extreme, there will be one absorption line occurring when the resonance condition is achieved. When the sample is axial, $g_x = g_y = g_\perp$, $g_z = g_{//}$, the absorption line will have 2 turning points. When the sample is rhombic, the EPR absorption line will have 3 turning

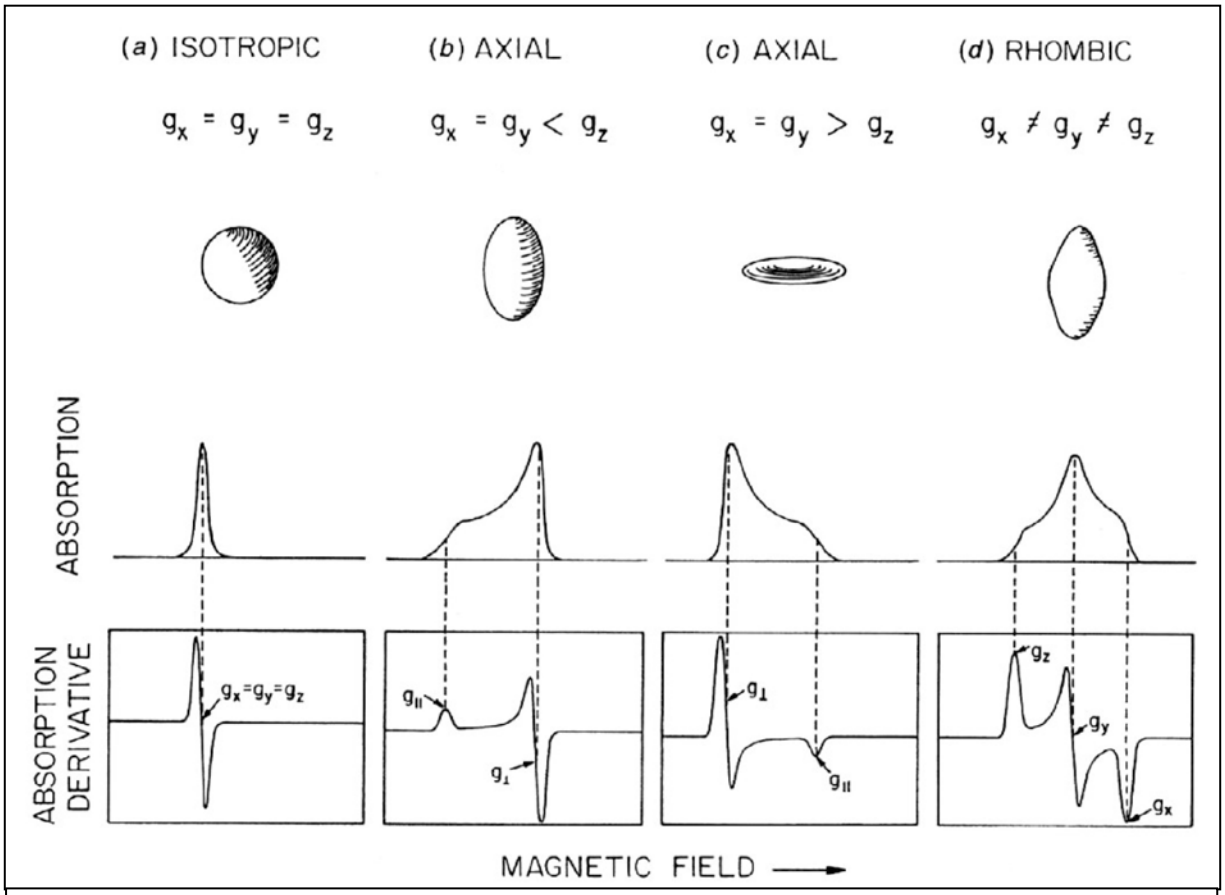

Figure 2-7 Idealized power EPR spectra of isotropic, axial and rhombic S=1/2 System.

points and generate a more complicated EPR derivative spectrum. (Figure 2-7)

The EPR signal line shape is not only determined by the outside magnetic field B_0 and the electron spin S. There are three types of interactions between two molecules that could perturb and split the signal (Figure 2-8): (a) Hyperfine interaction, which is between an unpaired electron and the nucleus where the unpaired electron resides. (b) Super hyperfine, is between an unpaired electron and a neighboring (ligand) nucleus. (c) Spin-Spin interaction, is between 2 unpaired electrons within a molecule.

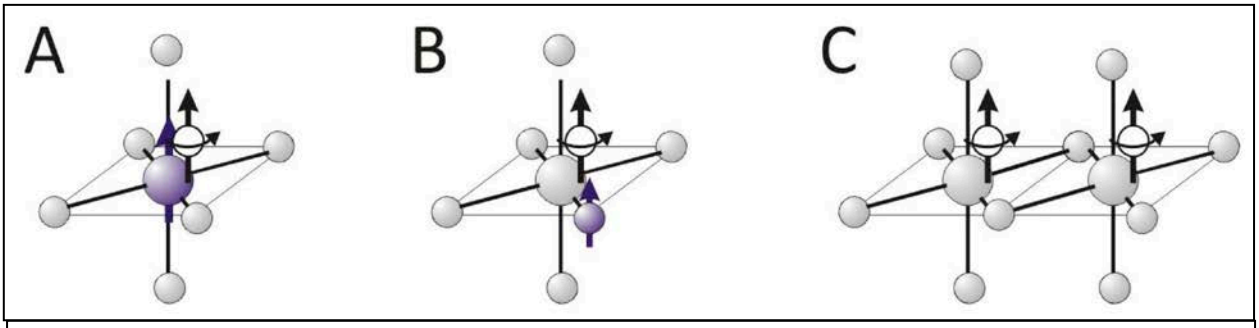

Figure 2-8 Three types of spin-spin interactions that can occur in protein samples

Only paramagnetic forms of metals ions are EPR active. And signal can be detected in the reduced form or the oxidized form, and sometimes in both. Samples are normally prepared using dithionite as a reductant or ferricyanide as an oxidant. This can already give a clue of which metal ion is present. For example, both redox states of Fe can potentially be EPR active, although the 2+ state normally is not. Most metal ions have unique spectra, the position of the g-value can indicate the presence of a high-spin system or not. And for S=1/2 systems when $g<g_e$, it indicates that the metal ion has less than half filled outer shells, alternatively, when $g>g_e$, the metal ion has more than half filled outer shells. The nuclear spins and the amount of unpaired electrons can affect the hyperfine splitting on the EPR spectrum, which can tell the origin of the

metal itself. Finally, superhyperfine interactions/splitting can also indicate the presence of ligands with a nuclear spin. The spectra for different types of Fe-S clusters are shown in Figure 2-9. There are 3 basic types of common Fe-S cluster: [2Fe-2S] clusters, [3Fe-4S] clusters, and [4Fe-4S] clusters. And only the EPR active ones can be detected. Such as, $[2Fe\text{-}2S]^{+}$ clusters, $[3Fe\text{-}4S]^{+}$ clusters, $[4Fe\text{-}4S]^{+}$ clusters and finally, the high-potential Fe-S cluster (HiPIP) $[4Fe\text{-}4S]^{3+}$. They also have different temperature behavior. Most of them can be detected in a specific temperature range. $[4Fe\text{-}4S]^{+}$ clusters can only been detected around 10K, and $[2Fe\text{-}2S]^{2+}$ clusters can only been detected around 20-70K.

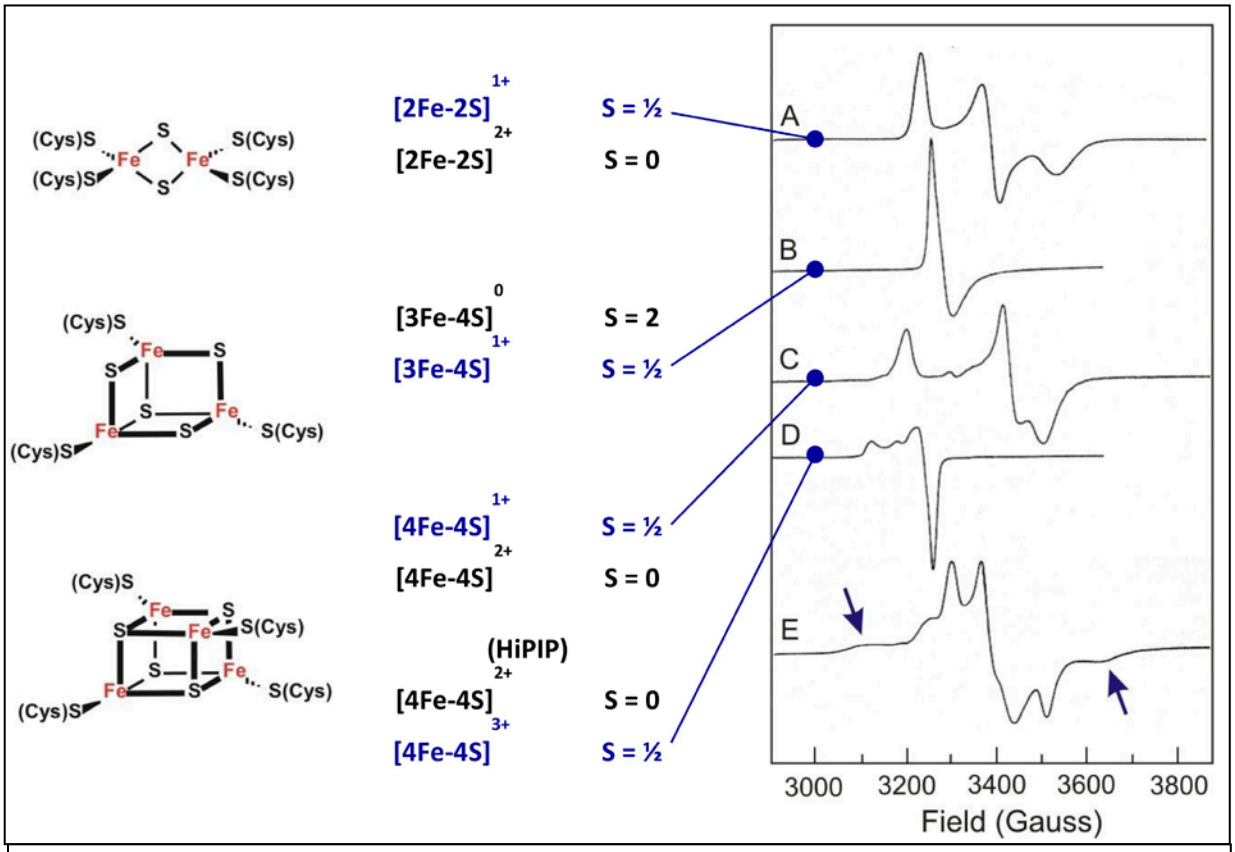

Figure 2-9 Overview of cluster types, allowed redox states and corresponding spin states and EPR spectra for common types of iron-sulfur clusters present in protein samples.

2.11.2. EPR measurement

EPR spectra were measured at X-band (9 GHz) frequency on a Bruker EMX spectrometer (Figure 2-10). 77 K data were obtained by using a liquid nitrogen finger Dewar inserted into the cavity. General conditions were: microwave frequency, 9.385GHz; microwave power incident to the cavity, 20dB; sweep: 280 mT to 360 mT, conversion time: 327 msec, time constant 327 msec. A water sample was measured under the same condition, and used as a blank control. By comparison of the double integral of the signal detected in the standard copper perchlorate (10mM $CuSO_4$, 2mM $NAClO_4$, 10mM HCl) with that of the signal measured under the same condition in the enzyme samples, the amount of signal (spin intensity) of the paramagnetic species can be calculated.

Figure 2-10 Bruker EMX spectrometer

Chapter 3: Results

3.1. Optimization of the IspH iron-sulfur cluster content

3.1.1. Expression and Purification

Nine cell lines were constructed (Table 3-1), and 8 of these showed similar growth rates. On average, each 1L of culture yielded about 10 g of wet cells. Only the cell line that contained the plasmid with IspH from *E. coli* and the ISC plasmids stopped growing after the addition of inducers. The whole growth/purification procedure was repeated 3 times, and the data obtained was averaged. Table 3-1 summarizes the behaviors of all the cell lines, including the data from expression, purification and iron determination.

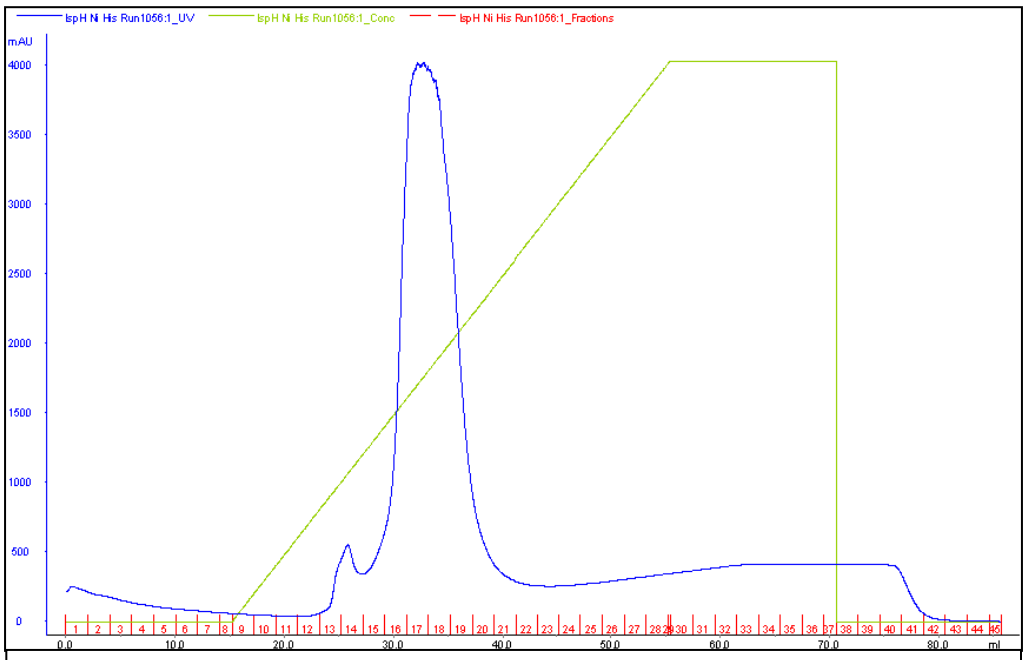

Figure 3-1 A typical purification graph

Run 1	Protein Collected (mL)	Protein Conc ((μM)	Iron Conc ((μM)	Cluster%	Average cluster%
Pf reg	4	49.3	41.09	20.8	26.8
Pf ISC	6	73.8	68.9	29.5	40.2
Pf ErpA	4	119.11	36.5	7.6 (ignored)	50.35
Aa reg	4	74.01	85.53	29.2	36
Aa ISC	4		n.d.		46.5
Aa ErpA	6	97.71	118.6	30.3	35.3
Ec reg	4	112.1	317.76	70.9	73.3
Ec ISC	4		n.d.		n.d.
Ec ErpA	4	8.57	16.78	48.9	42.2
Run 2	**Protein Collected (mL)**	**Protein Conc ((μM)**	**Iron Conc ((μM)**	**Cluster%**	**Average cluster %**
Pf reg	4	257.36	109.09	10.6	26.8
Pf ISC	6	224.34	388.79	43.3	40.2
Pf ErpA	4	95.59	222.95	58.3	50.35
Aa reg	4	133.4	217.78	40.8	36
Aa ISC	4	57.83	114.03	49.7	46.5
Aa ErpA	6	115.55	286.2	26.5	35.3
Ec reg	2	109.79	338.52	77.1	73.3
Ec ISC	4		n.d.		n.d.
Ec ErpA	6	115.55	118.3	25.6	42.2
Run 3	**Protein Collected (mL)**	**Protein Conc ((μM)**	**Iron Conc ((μM)**	**Cluster%**	**Average cluster %**
Pf reg	2	123.75	242.815	49.1	26.8
Pf ISC	4	131.727	245.187	48	40.2
Pf ErpA	4	127.596	223.6	42.4	50.35
Aa reg	6	223.448	336.945	38	36
Aa ISC	2	53.67	92.89	43.3	46.5
Aa ErpA	8	154.779	304.28	49.2	35.3
Ec reg	2	121.063	347.938	72	73.3
Ec ISC	2		n.d.		n.d.
Ec ErpA	4	42.432	88.44	52.2	42.2

Table 3-1 Optimazation of the IspH cluster content result

IspH was purified from the 8 remaining cell lines. The purification procedure was as described in chapter 2. The *E. coli* and *P. falciparum* enzymes were purified on a Ni-affinity column. The procedure was the same for the *A. aeolicus* enzyme, however a heat treatment was added to the procedure before the enzyme was loaded onto the column. A typical purification profile is shown in Figure 3-1. The IspH can be easily recognized due to the brown color of the fractions and in general no other method like assaying the activity is needed to confirm this.

3.1.3. UV-absorption and Iron determination

The identity and purity of the IspH enzymes was established by running a SDS-PAGE (Figure 3-2). IspH has a molecular weight of 32 kDa. In the figure, CE stands for cell extract, 1st and 2nd indicating the fractions from the purification which have the UV absorption, and FT stands for flow through, means the solution after the column. As shown in the figure, the second peak shows a band at around a molecular weight of 32kDa, indicating the presence of IspH in >90% purity. The protein fractions containing IspH were pooled and stored in the anaerobic tent at room temperature for further use. The different proteins showed very different stability at room temperature. The *A. aeolicus* and *P. falciparum* enzymes precipitate after only 1-2 days. The *E. coli* enzyme is stable for several weeks.

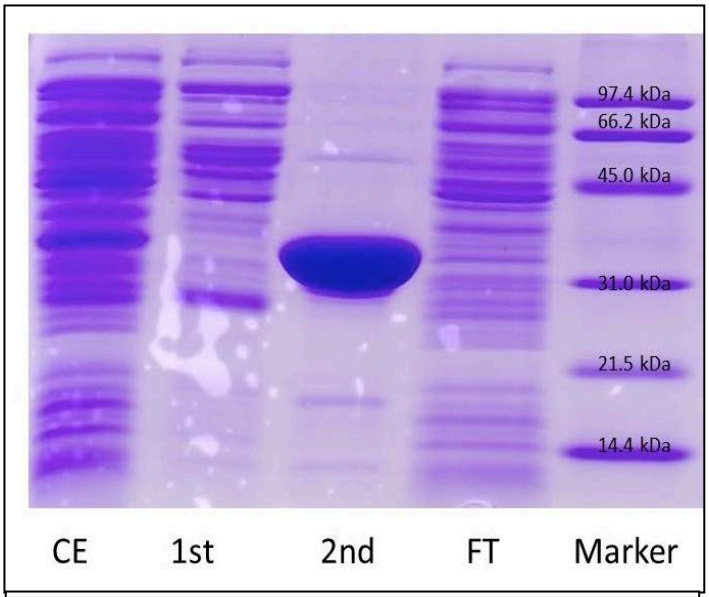

Figure 3-2 A typical SDS-page gel

3.1.3. UV-absorption and Iron determination

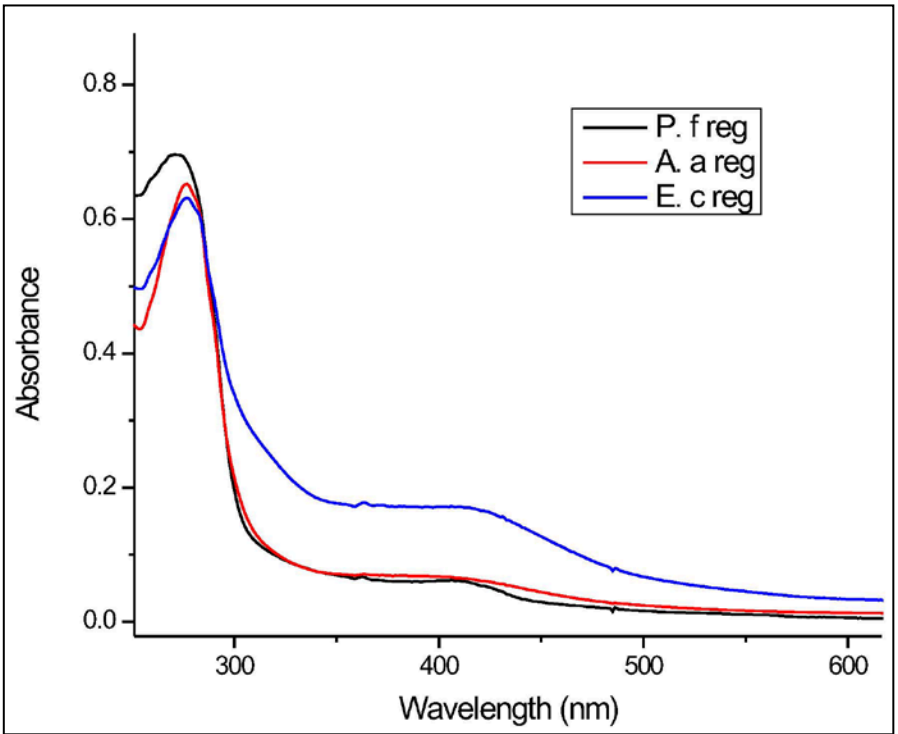

Figure 3-3 Typical spectra for the three IspH enzymes

Typical absorption spectra for the different IspH enzymes are shown in Figure 3-3. The 280 nm band is due to the protein itself. The broad band at around 420 nm indicates the presence of $[3Fe\text{-}4S]^{1+}$ or $[4Fe\text{-}4S]^{2+}$ clusters. A band at 310 nm would indicate the presence of single iron ions, which can be the indication for cluster breakdown during the purification procedure. There is no obvious band present at this region. Upon addition of dithionite, the 420 nm band disappears due to the reduction of the clusters. A peak at around 330nm peak indicates the presence of reduced dithionite (data not shown).

After every purification, as described in the former chapter, besides six standard iron samples, 3 samples with different concentrations of each protein were prepared. The linear plot for the iron is shown in Figure 3-4. The iron concentration of the protein samples was determined from comparison of the absorption obtained for each sample with the absorption obtained for the iron standards. The iron and cluster content for each protein sample is listed in Table 3-1.

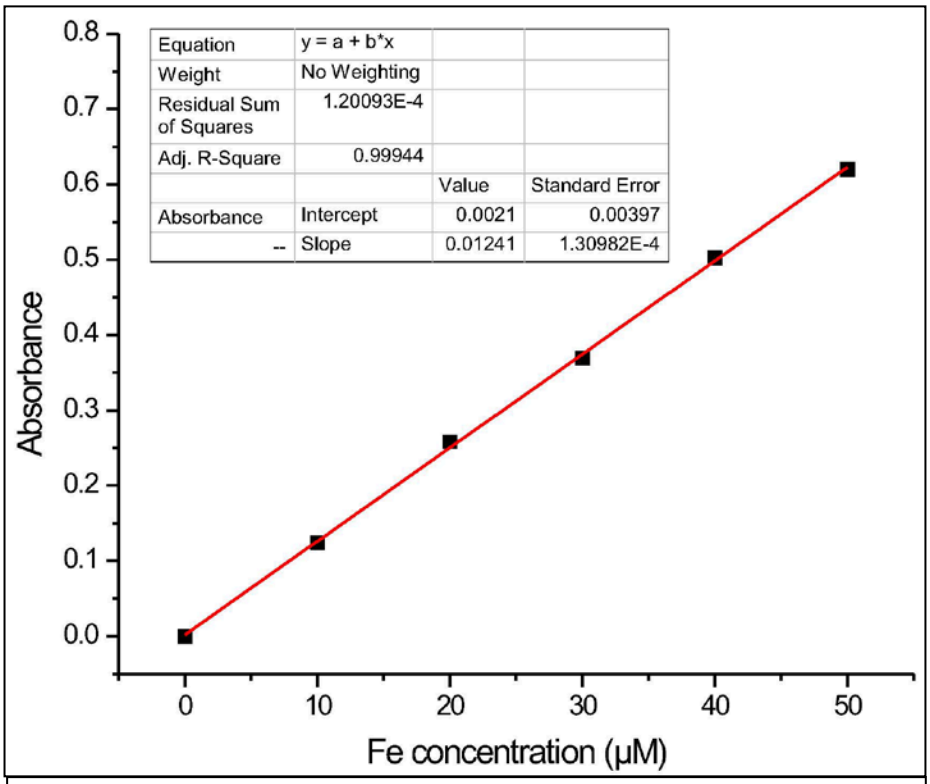

Figure 3-4 A typical iron standard plot created by the standard iron which had been incubated with the samples together as controls

The main reason to perform these studies were the finding by previous studies that the protein samples from all three different organisms would only have about 15% cluster content. To minimize the amount of protein needed for advanced EPR and Mössbauer studies it would be important to increase the cluster content significantly. For ENDOR measurements the cluster reconstitution procedures worked well, however, the black iron precipitate that is formed during this procedure sticks to the protein samples and would interfere with the interpretation of the Mössbauer spectra.

The cluster content for IspH from *A. aeolicus* and *P. falciparum* did increase in the presence of the ISC or the ErpA proteins. As for the *E. coli* cell, it possessed already 70% cluster without these accessory genes, which is significant improvement in comparison with the data obtained by Dr. Weiya Xu. Her sample contained an average of 20% cluster content. The *E. coli* samples have the darkest color and highest 420 nm verses 280 nm absorbance ratio during 20 times

repeats. Therefore IspH from *E. coli* was selected for the advanced spectroscopic studies. However, the expression of *E. coli* IspH in the presence of the ISC proteins failed to form IspH protein in more than 5 repeats. Co-expression with the ErpA protein did not improve the cluster content, 42%. Co-expression of *E. coli* IspH with both the ISC and ErpA protein is planned for the near future. For now the 70% cluster content of IspH from *E.coli* is good enough start our kinetic and Mössbauer experiments.

3.2. Kinetic and EPR-detected freeze-quench studies

For this part of the project we studied four types of protein samples: *A. aeolicus* wild-type IspH, *A. aeolicus* E126Q and H124F mutant IspH, and *E.coli* wild-type IspH. The aim is to assign the different forms that have be detected by our and other groups as true reaction intermediates, alternative intermediates, true products, and/or dead-end products.

3.2.1. Colorimetric Assay

Reduced methyl viologen was used in all our experiment as the electron donor. Reduced methyl viologen has a blue color and become colorless when it is oxidized. The absorbance band at 603 nm has an extinction coefficient of 1.36×10^4 $M^{-1}cm^{-1}$. Note that the reaction requires two electrons and methyl viologen can only donate 1e at-a-time. Therefore the speed of the oxidation of methyl viologen detected is two times faster than the reaction rate of the enzyme.

(a) *A. aeolicus* Wild Type and Mutant IspH

The activity for wild-type IspH from *A. aeolicus* wild type was studied. The measurements were repeated twice. The average values for the k_{cat} and the K_M were 0.174 ± 0.015 s^{-1} and 16.7 ± 5 μM, respectively. This means that cycle of the reaction takes about 5.73 seconds (Table 3-2), which is consistent with previous studies (11). Since the cluster content was 32%, the hypothetical k_{cat} for fully active enzyme was 0.544 ± 0.047 s^{-1}.

The activity for the H124F and E126Q mutant IspH from *A. aeolicus* was different from earlier studies. For the H124F mutant the activity is very low, even when 1 mM protein (ultimate option) was used. With 1 mM enzyme the V_{max} is 1.31×10^{-3} s^{-1} with 69% cluster content, after the correction, the V_{max} is 1.90×10^{-3} s^{-1} which is still somewhat lower than previously reported, 3.34×10^{-3} s^{-1}.

The activity for the E126Q mutant is even harder to detect. With 1 mM enzyme, the color in the cuvette will not change over a 1 hour period. This would indicate that this mutant is inactive. Some activity was reported previously. We assume that since these earlier kinetic studies were performed outside an anaerobic tent or box, small trace of oxygen might have affected the results.

(b) *E. coli* Wild Type

Besides the fact that the IspH from *E. coli* has much higher cluster content, the activity was much higher too. We calculated a k_{cat} of 1.07 ± 0.08 s^{-1}, and a K_M of 4.9 ± 1.3 μM (Table 3-2).

This means that one cycle of the reaction will be finished within 0.930 seconds under the used measuring conditions. Since the cluster content is 86%, the corrected k_{cat} was 1.244 ± 0.009 s^{-1}.

Enzyme	Cluster content (%)	Enzyme activity after correction for cluster content (s^{-1})	K_M(µM)
IspH from *A. aeolicus*	32	0.54±005	16.7±5
IspH from *E. coli*	86	1.24±0.09	4.9±1.3
A.a. H124 F mutant	69	$1.9x10^{-3}$	n.d.
A.a. E126Q mutant	54	n.d.	n.d.

Table 3-2 Kinetic study result (n.d., not detected)

3.2.2. Rapid freeze quench study

Here a selection of the obtained data will be presented. All runs have been repeated several times. Some of the runs have been repeated more than 10 times. This is because we needed to test the new Kintec machine, but also to figure out what condition would provide the best signal intensities. We also had HMBPP preparation with different purities and different runs were needed to make sure the impurities did not interfere with the reaction. Currently we are able to make good quality HMBPP preparations and this is not a problem anymore.

3.2.2.1. Pre and Steady-state Experiments

One reaction cycle for *A. aeolicus* IspH takes 5.7 seconds, and for *E. coli* IspH it takes less than 1 second. Based on this it is clear we need a rapid method to study these reactions: Enzyme in

the presence of excess dithionite was mixed with 10 equivalents of substrate, incubated for a short period, and the reaction was quenched by rapid freezing. It is was assumed that the reaction under these conditions should be done in ~1 minute for *A. aeolicus* IspH and 10 second for *E. coli* IspH.

(a) *A. aeolicus* Wild Type

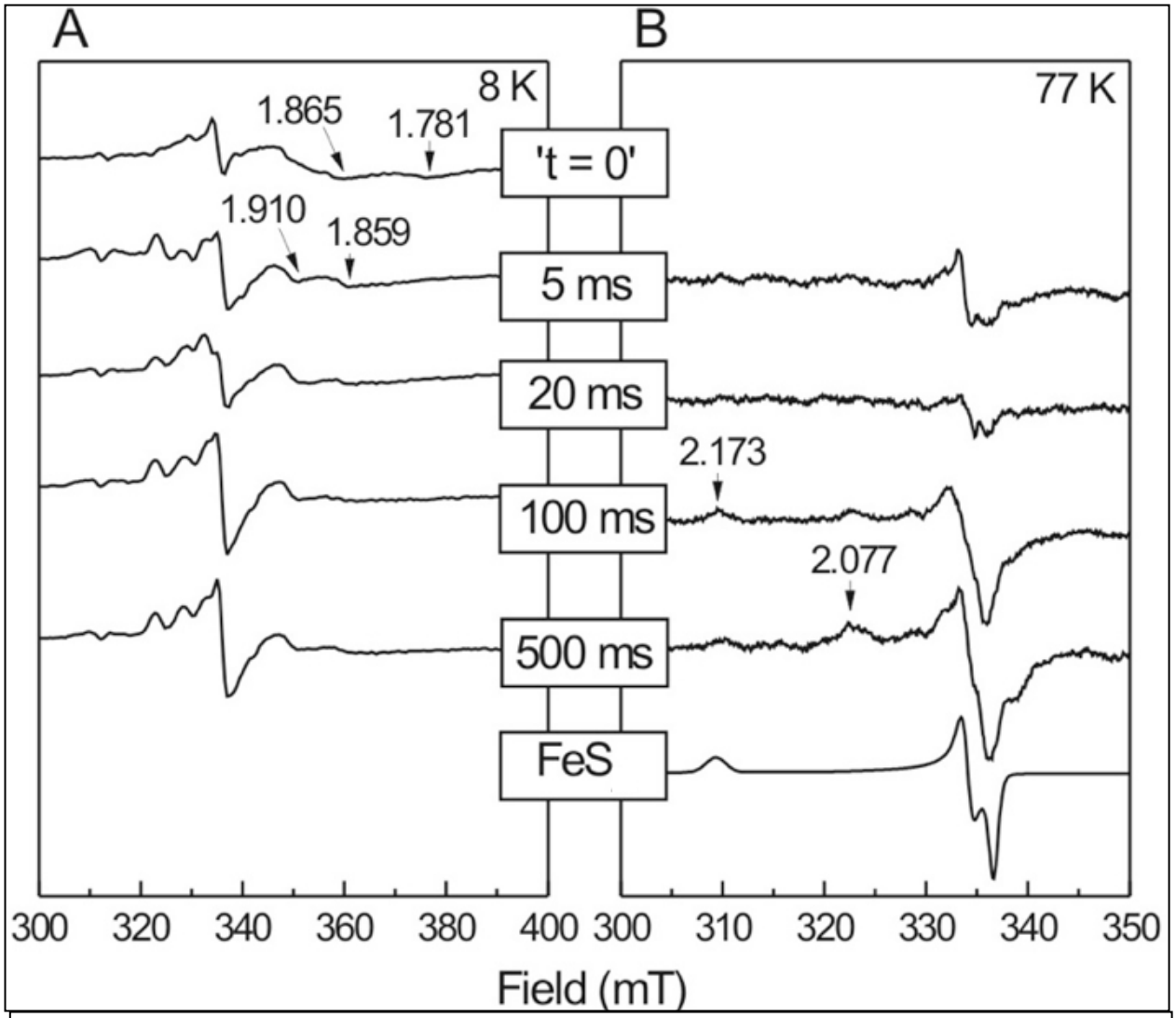

Figure 3-5 *A. aeolicus* IspH WT freeze-quench results (set 1)
Final concentration: Enzyme: 420 µM (Cluster: 126 µM) Substrate: 5 mM Dithionite: 33 mM

The result for *A. aeolicus* WT is shown in Figure 3-5. The FeS_I species with g-values of 2.176, 2.008, and 2.000 is detectable in the 100 ms spectrum at 77 K. A second signal with g-values 2.077, 2.004, and 1.993 also develops at around the same time. Due to similarities to a signal that can be induced by incubating IspH with IPP we assign this signal to the formation of a cluster-bound product species (28). However since a full reaction cycle should take about 6 s as the kinetic study suggested, it could also be another reaction intermediate. The data indicates that the FeS_I species is kinetically competent since it forms within 40 ms. In order to prove that the FeS_I species is a transient intermediate, this signal should first accumulate and then disappear when the reaction runs out of substrate. All tubes were also measured at 8 K to detect what happens to the $[4Fe\text{-}4S]^{1+}$ cluster. The cluster signal can easily be detected in a regular reduced sample but is absent already in the 4.6 ms sample indicative for a rapid oxidation of the cluster when the enzyme is mixed with substrate (data not shown). For all freeze-quench runs shown in this dissertation, the EPR samples were measured at different temperatures. The unique cluster-bound intermediate or product species can be detected without saturation in the 50 to 100 K range while the regular reduced 4Fe cluster is detectable without saturation at 6 to 10 K. In all cases the samples show that the 4Fe signal is not detectable anymore as soon as (4.6 ms) the samples are mixed with substrate. We will only show the 77 K data in the remainder of this chapter.

Several freeze-quench runs were conducted with WT enzyme. The goal was to detect the time-point where the FeS_I species would start to disappear again. Figure 3-6 shows a set of spectra where the longest incubation time was 90 min. The FeS_I signal was still detectable after this long incubation time. It is not clear what is going on. This data could indicate of course that the FeS_I

species is not a reaction intermediate. It is also possible that the enzyme inactivates rapidly and gets stuck in the FeS_I form. It is more likely, however, that the use of dithionite as reductant instead of methyl viologen could slow down the reaction considerably. Studies with the other

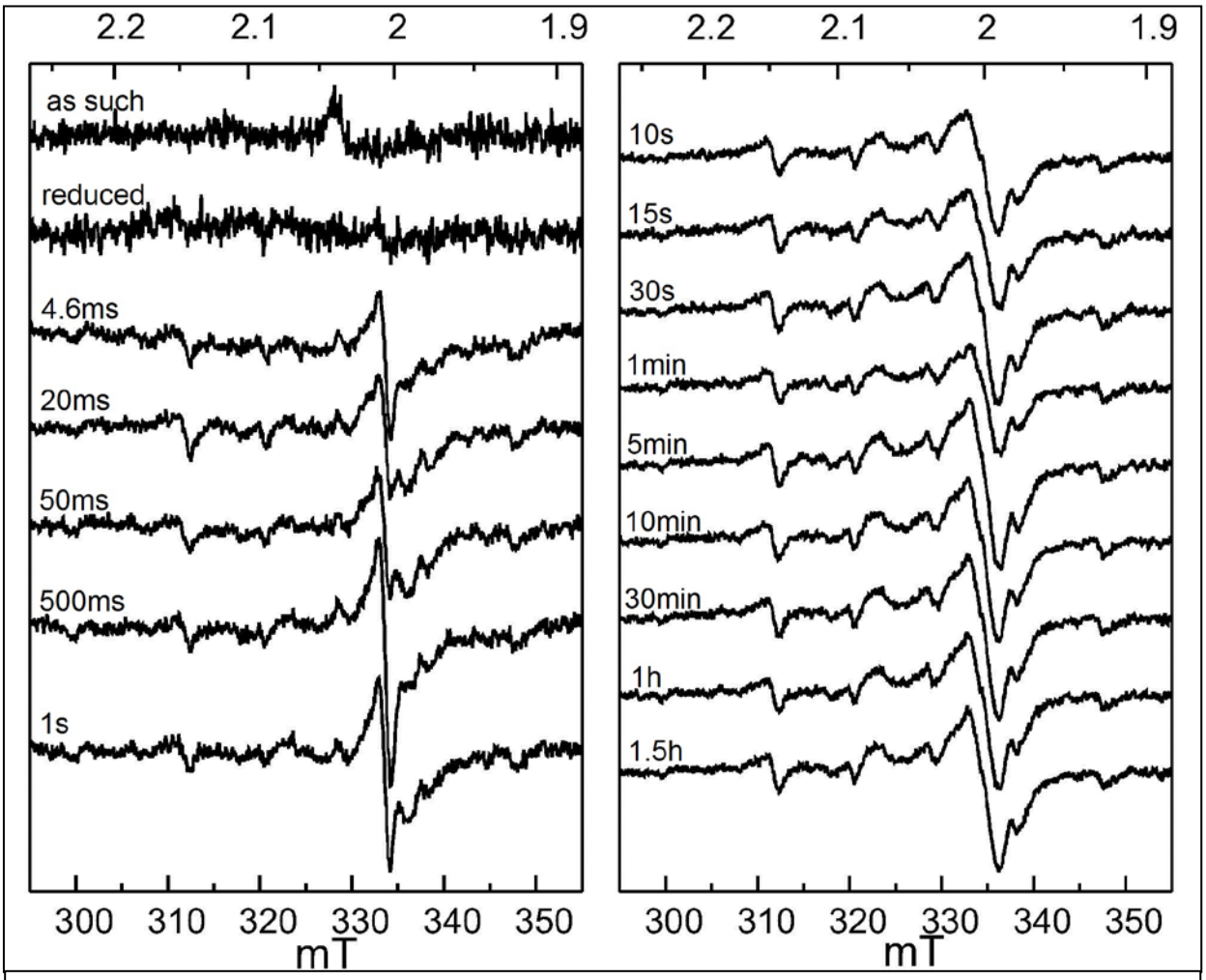

Figure 3-6 Kinetic studies with *A. aeolicus* IspH WT enzyme (set 2). Concentrations in sample: Enzyme: 286 µM (Cluster: 150 µM), Substrate: 1.5 mM, Dithionite: 33 mM

cluster-containing enzyme from the DOXP pathway studied in this lab, IspG, showed that methyl viologen can speed up the reaction 1000 times in comparison with dithionite (29). Methyl viologen is not being used in the EPR detected freeze-quench studies because of its large radical signal. For comparison we need to develop an assay, NMR or mass spectrometry based, that can

provide the values of V_{max} and K_m with just dithionite as the reductant. A mass spectrometry-based assay already proved that only dithionite is needed for the reaction to proceed (11). Unfortunately we were not able to do the assay at the mass spectrometry facilities here in our Department. Efforts are under way to use the facilities in the Department of Pharmacal Sciences.

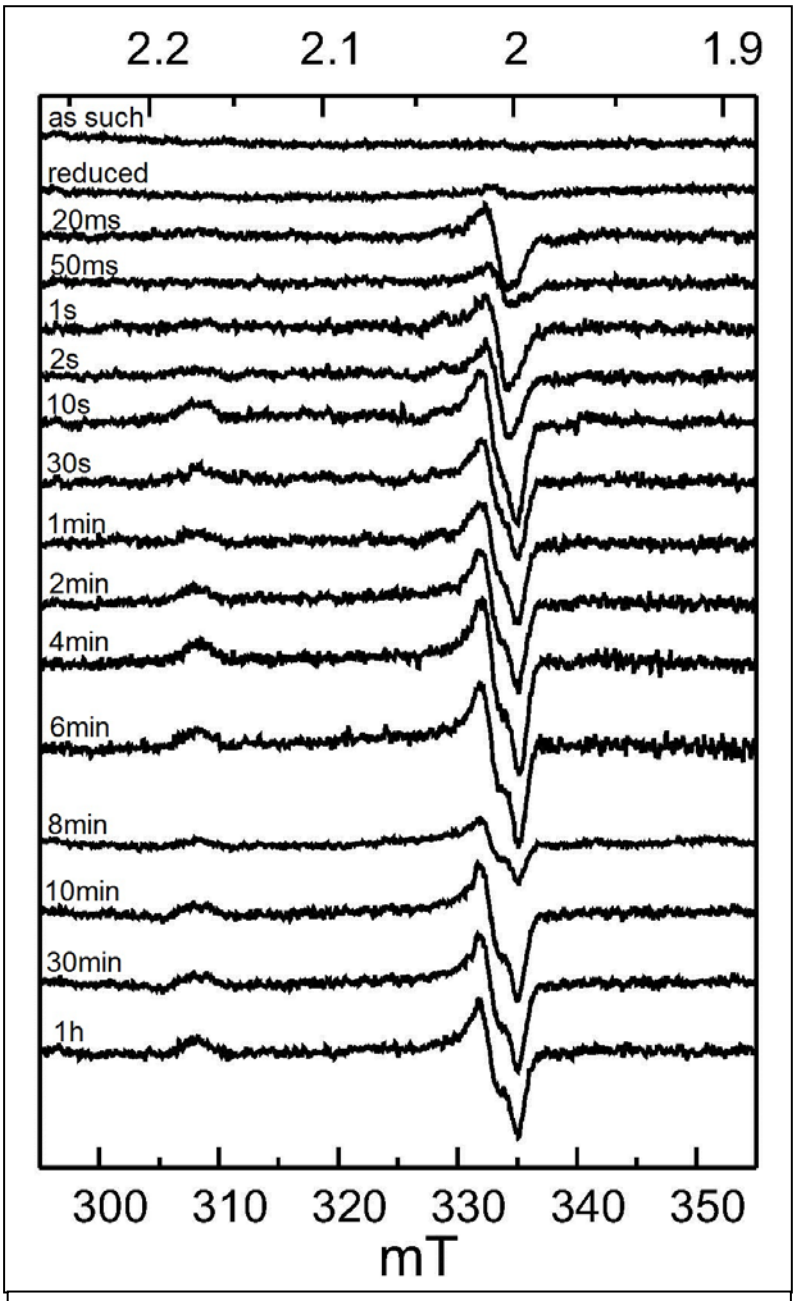

Figure 3-7 Spectra obtained for *E. coli* IspH WT. Concentrations in sample: Enzyme: 312 µM (Cluster: 150 µM), Substrate: 1.5 mM, Dithionite: 33 mM

(b) *E. coli* Wild Type

Experiments were also performed with WT IspH from *E. coli*. The results are shown in Figure 3-7. Also here we used a 10x excess of substrate and again the FeS_I develops but does not disappear within the times tested.

3.2.2.2. Single turn over experiment

Another strategy we tried is to only add 1 equivalent of substrate to enzyme. First, this can save a lot of substrate. Second, monitoring of the formation of intermediates and possibly product-based signals in a single turnover cycle would give us an actual reaction time under the condition used: dithionite instead of methyl viologen as the electron donor.

(a) *A. aeolicus* Wild Type and Mutants

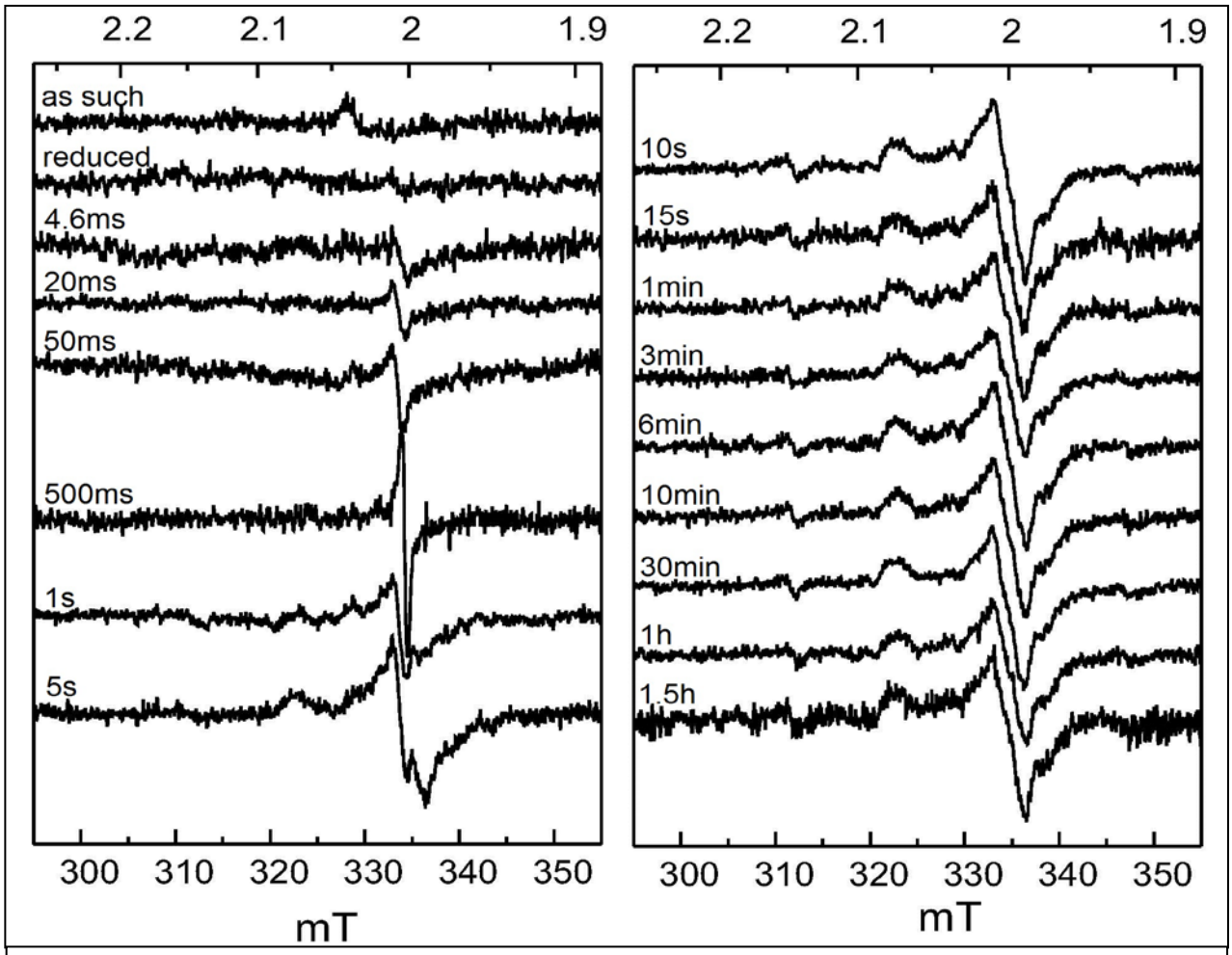

Figure 3-8 *A. aeolicus* IspH WT single turnover experiment
Final concentration: Enzyme: 286µM (Cluster: 150µM) Substrate: 150µM Dithionite: 33mM

The data for WT IspH from *A. aeolicus* is shown in Figure 3-8. Under these condition it appears that the FeS_I species is not detectable. A new signal with g-values of 2.074, 2.003 and 1.989 was detected instead. This signal appeared at 5 second and was still present after 90 min.

The same studies were also performed with mutant IspH to see of any of the species observed by us and other groups are kinetically competent. Spectra for the *A. aeolicus* E126Q mutant were obtained ranging from 4.6ms to 10 min. As shown in Figure 3-9, the characteristic signal with g-values of 2.117, 2.003 and 1.964 started to develop after 4.6 ms, increased intensity and then stayed detectable all the way up to 10 min.

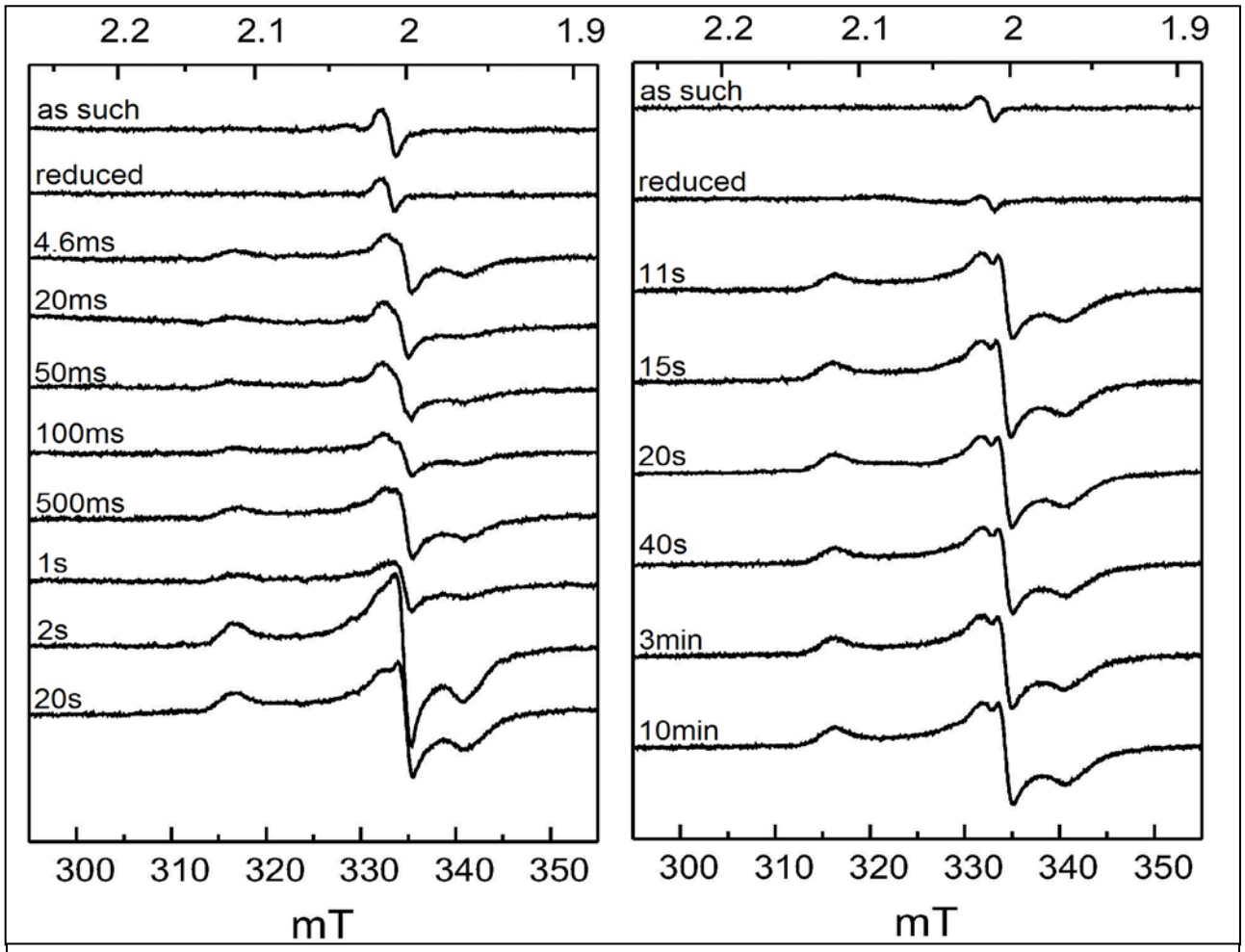

Figure 3-9 *A. aeolicus* IspH E126Q mutant single turnover experiment
Final concentration: Enzyme: 300 µM (Cluster: 150 µM) Substrate: 150 µM Dithionite: 33mM

Spectra obtained for the *A. aeolicus* H124F Mutant are shown in Figure 3-10. No FeS_I signal was detected, but instead a radical signal was present in the 20 ms to 1 min time range. A product-like signal with a g-values of 2.079, 2.004, and 1.989 appeared after 4 min and stayed the rest of the run all the way up to 90 min.

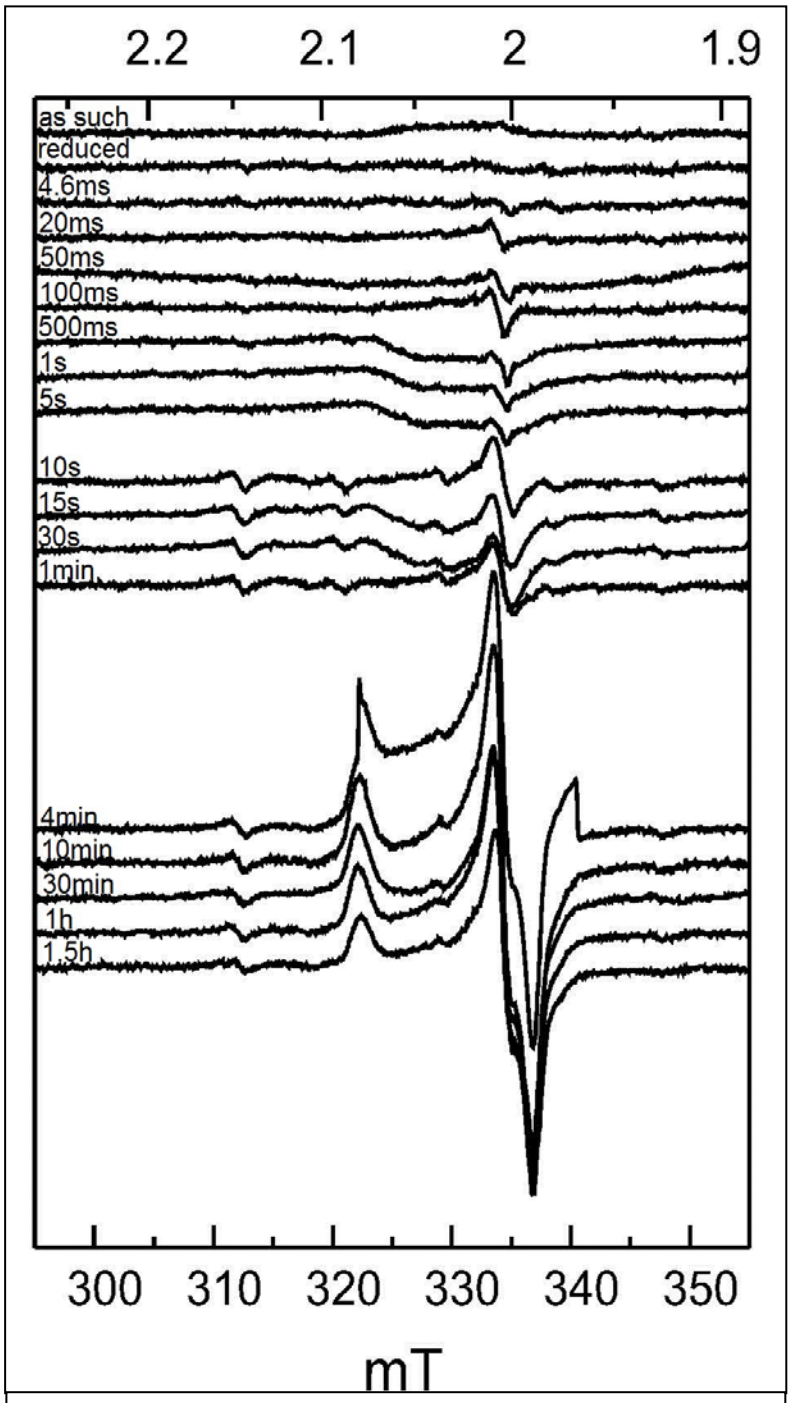

Figure 3-10 *A. aeolicus* IspH H124F mutant single turnover experiment
Final concentration: Enzyme: 210µM (Cluster: 150µM)
Substrate: 150µM Dithionite: 33 mM

(b) *E. coli* Wild Type

The single-turn-over data for WT IspH from *E. coli* is shown in Figure 3-11. A somewhat different result is obtained which is more in line with what we were expecting. Now the FeS_I is detected early in the reaction which then disappears and then a second signal can be detected which we attentively assign to cluster-bound product.

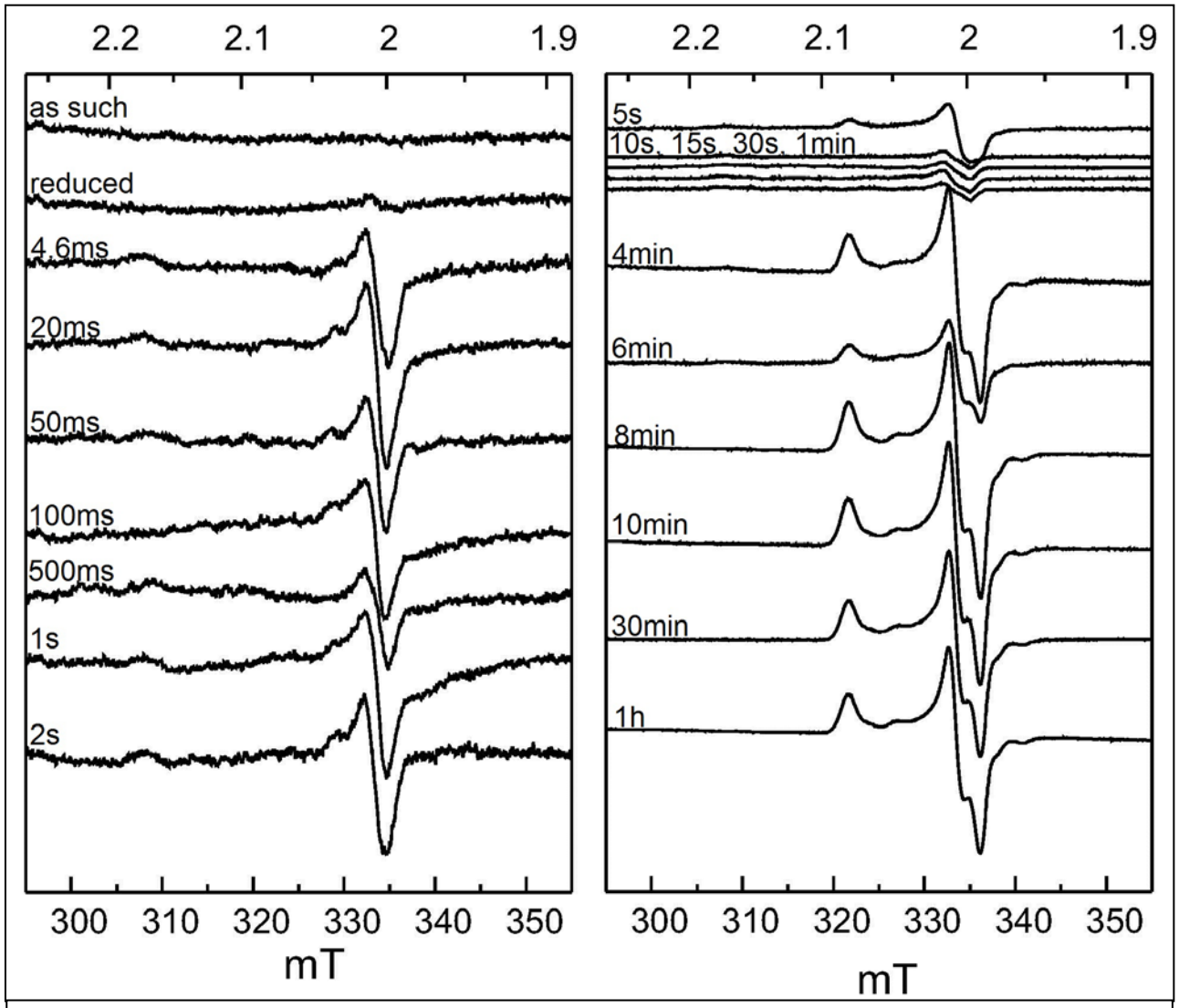

Figure 3-11 *E. coli* IspH WT single turnover experiment
Final concentration: Enzyme: 312 µM (Cluster: 150 µM) Substrate: 150 µM Dithionite: 33mM

3.2.2.3. One Electron-reduced IspH

We assumed that the [4Fe-4S] $^{2+}$ cluster in the IspH enzyme obtains the first electron from a donor like the flavodoxin/flavodoxin reductase/NADH system *in vivo*, or an artificial donor such as photoactivated deazaflavin or dithionite *in vitro*. The reduced [4Fe-4S]$^{1+}$ form binds HMBPP through its hydroxyl group and a HiPIP-like intermediate is generated. Now the enzyme is in an allyl anion-[4Fe-4S]$^{3+}$ form. When this form obtains another electron (plus hydrogen), the reaction would proceeds towards product generation. By pre-reducing the Fe-S cluster with treatment with dithionite and subsequently removal of the excess dithionite, we create a situation where the reaction can only go through the first redox step and reaction will stall. Under these conditions the reaction intermediate should accumulated without disappearing.

Previously, Dr. Weiya Xu was successful in making one-electron reduced IspH and capturing the FeS_I signal. After the incubation of the enzyme with excess dithionite for 15 min the cluster should be in the reduced form, then by running the samples through a PD10 column, excess dithionite was removed and the enzyme remained reduced. This was confirmed by the UV-visible absorption data (the 420 nm band indicates the oxidative status). After incubation of these one-electron-reduced enzymes with HMBPP, the FeS_I signal was detected in EPR spectroscopy. (Figure 1-21, 1-23)

However, this was not consistent with our recent observation. The IspH WT from *E. coli* did not remain reduced after the incubation and removal of the excess dithionite. And no FeS_I signal was captured by freeze quench and EPR measurement. An alternative approach was used to obtain one-electron reduced enzyme. Titanium(III) citrate was used as the reductant. Instead of the

PD10 procedure we opted to add 1 equivalent of this strong reductant. This compound has both a brown color causing an additional band in absorption spectroscopy (Figure 3-12) as well as an EPR signal. The EPR spectrum of the one-electron-reduced enzyme now shows an extra peak around g = 1.95. Fortunately, the FeS_I can be easily detected and this is consistent with the other studies.

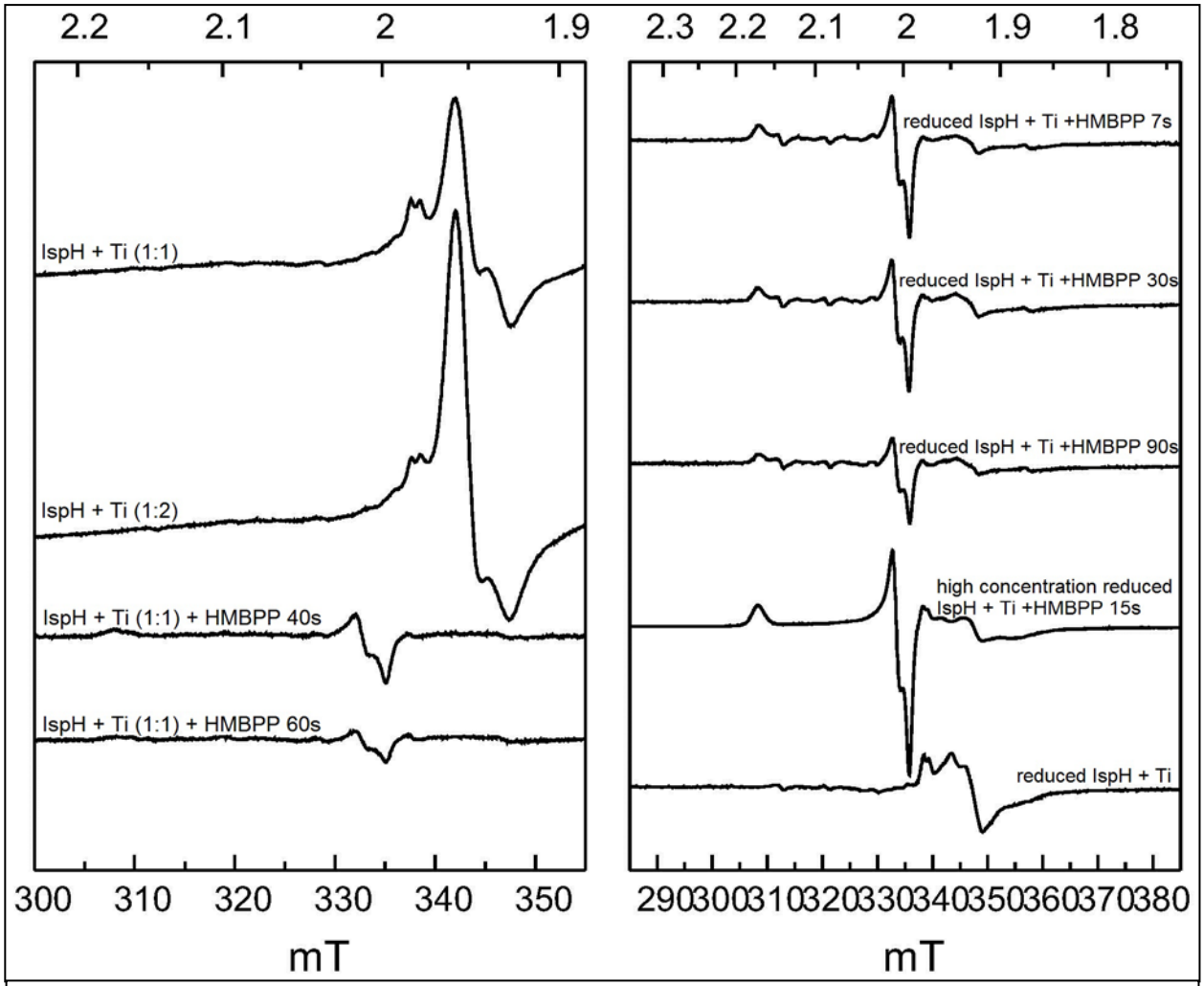

Figure 3-12 *E.coli* IspH WT one-electron-reduced experiment
Final concentration: Enzyme: 361µM (Cluster: 212µM) Substrate: 212µM

Chapter 4: Discussions

4.1. Optimization of the IspH iron-sulfur cluster content

Earlier studies from our group were done with WT and mutant IspH from *A. aeolicus*, and WT IspH from *P. falciparum* and *E. coli*. Both as-isolated protein and protein after cluster reconstitution were used. There are several reasons why this was not a good situation.
1) With a cluster content of only 20%, much more protein is needed to obtain a good signal with EPR measurements as well as future Mössbauer measurements. 2) Although it is assumed that the enzyme without cluster does not participate in the reaction. It cannot be excluded that it could still bind substrate which would change the observed parameters. With this in mind, the higher the cluster content, the more we can trust the obtained values. 3) The reconstitution only results in 50-60% cluster content and also introduces other Fe species detectable as a darker color of the protein sample. Some of this can be removed but some appears to stick to the enzyme.

Here we focused on improving the iron-sulfur cluster content in naturally formed IspH with the help of the iron-sulfur cluster biogenesis system ISC and an A-type carrier protein ErpA. IspH from three different sources, *A. aeolicus, P. falciparum*, and *E. coli*, was expressed by itself, or co-expressed with the iron-sulfur cluster biogenesis system or the A-type carrier protein ErpA. The different combinations resulted in 9 different cells strains. Each strain was grown in culture

and when possible the IspH was isolated. For each IspH sample the protein and iron concentrations were determined and the cluster content was calculated.

The obtained data is not what should be expected. Although negative results are normally not reported in the literature, there are several reports about successful expression of iron-sulfur-cluster containing enzyme when coexpressed with the *isc* genes. For the *P. falciparum* enzyme there is a clear increase, from 27 % to 40 % when the *isc* genes are coexpressed. This number further increases when the ErpA enzyme is coexpressed (50 %). One would expect that having both *isc* and *erpA* genes present could further increase the cluster content. Efforts are under way to make a duet vector that includes both the *isc* and *erpA* genes. For the *A. aeolicus* enzyme there is also an increase in content, from 36 % to 47 %, when the enzyme is coexpressed with the *isc* genes. There is no effect when ErpA is coexpressed. It is not clear why this is, but the *E. coli* ErpA might not recognize the IspH from *A. aeolicus*. The *E. coli* enzyme showed a remarkable high cluster content expressed all by itself: 73%. Similar amounts were measured in 20 repeats. This is much higher than the earlier reported ~20% cluster content. Problems arose, however when the enzyme was coexpressed with the other genes. Coexpression with the ErpA enzyme caused a lower cluster content (42 %). Coexpression with the Isc enzymes caused problems with cell growth. The cells grew well initially but grew much slower after the addition of inducer. It is not clear why. Changes in growth temperature and amount of inducers did not solve this problem. When the amount of inducer were reduced from 3 g down to 1.5 g, 1 g, 0.5 g, and even 0 g, the cells grows better. Under normal condition this cell line needs 9-10 hours after the addition of the inducer to reach the harvest point. With less inducer, the cell can reach the needed weight within 5 hours; however, the purification did not obtain any IspH protein. The reduction

of the temperature did not help either; the cells grow very slow and did not form any IspH protein.

4.2. Kinetic and rapid-freeze quench measurements

4.2.1. Kinetic study

The goal of the work described here was to put the discovered EPR active species in the frame work of the actual reaction mechanism. Unfortunately, it turned out that the reaction rate of the reaction is much slower in the presence of dithionite, as opposed to methyl viologen as electron donor/mediator. Therefore the turn-over numbers obtained in the colorimetric assay cannot be used for direct comparison. Still some important findings can be reported. We are currently working on an NMR- or mass-spectrometry-based assay to obtain turn-over numbers for the reaction in the presence of dithionite only.

4.2.2. Reaction

4.2.2.1. FeS_I signal

As for WT IspH from *A. aeolicus* and *E. coli*, similar results were obtained in pre-steady state experiment (Figs. 3-5, 3-6, 3-7). However, the signal-to-noise ratio for the sample made with the *A. aeolicus* enzyme is too low to draw any strong conclusions. The cluster content in this enzyme is clearly too low to obtain good data. In both experiments, however, the FeS_I signal was

detected and it stayed detectable after it formed which would argue against it being a reaction intermediate. However, in the single-turn-over experiment with *E. coli* enzyme (Fig. 3-11), the FeS_I signal forms and disappears which is in line with it being an intermediate in the reaction. The disappearance went along with the rises of a new paramagnetic species which we assigned to the 'product' signal. The single-turn-over experiment with *A. aeolicus* enzyme (Fig. 3-8) is differed from the ones gotten with *E. coli*. Most likely we suffer again from low cluster content and signal intensity. This also makes other background signals like a radical-type signal around 500 ms more intense. It is important to notice, however, that although the FeS_I signal is not detectable the 'product' signal is which indicates that the reaction much have taken place and the FeS_I signal was just lost in the noise. Parallel experiments, however, will be needed to prove that this is indeed the case. The quickest way would be to improve the signal intensity or alternatively show the formation of IPP and/or DMAPP using NMR or Mass spectrometry based experiments.

In the single-turn-over experiment with the H124F IspH mutant from *A. aeolicus* the formation of a radical-like signal was detected instead of the FeS_I formation. Previously, the H124 residue was proposed to have a role in the binding the pyrophosphate group of the substrate HMBPP, as well as holding the substrate in the appropriate orientation to fulfill the catalytic reaction. This was based on the fact that the $[4Fe\text{-}4S]^+$ still disappears but a radical signal is detected. And this is consistent with our recent study. However, the same 'product' signal is detected after 4 min which indicates that some reaction did take place. It also put the origin of the 'product' signal in doubt. Again parallel experiment are needed to see what 'product' has been formed if any.

4.2.2.2. The E126Q species

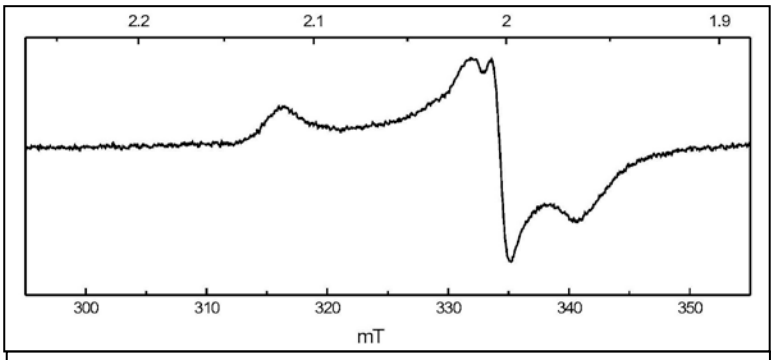

Figure 4-1 EPR signal obtained for the E126Q mutant

The *A. aeolicus* E126Q IspH mutant was a completely inactive protein. The EPR signal (Figure 4-1) was very clear and stable from 4.6ms to 10 min. As suggested by Oldfield's group, E126 stabilizes the HMBPP C_4-OH through a water network, which caused the rotation of the hydroxyl group, and should play a role in the dehydroxylation. Mutation of this residue makes this reaction impossible. The rapid freeze quench result appears to be in line with this proposal. This signal appears to form a fast as the FeSI signal, however, and it therefore kinetically competent and could be the first reaction intermediate as proposed in the bio-organometallic model (Fig. 1-18). More time points are needed to be able to calculate the speed of formation of both the FeS_I and this E126Q signal.

4.2.2.3. Product signal

Previously, only experiments with the one-electron-reduced enzyme were conducted, and both the FeS_I and the E126Q signals were discovered. It is not clear how both signals fit into the reaction mechanism. In this thesis, with the supply of excess electron donor, and a longer time frame intended to capture the complete cycle of the whole reaction, a product-like signal was observed in several of the experiments.

In the study of WT IspH fom both *A.aeolicus* and *E. coli*, as well as the IspH H124F mutant, signals with very similar g values were obtained (Figure 4-1). It is surprising that this 'product' signal is detected in the H124F mutant. This could be the result of the fact that dithionite is the limiting factor in these assays and under those conditions the H124F mutant is almost as slow as the WT enzyme in forming product. However, without further study, this conclusion cannot be confirmed.

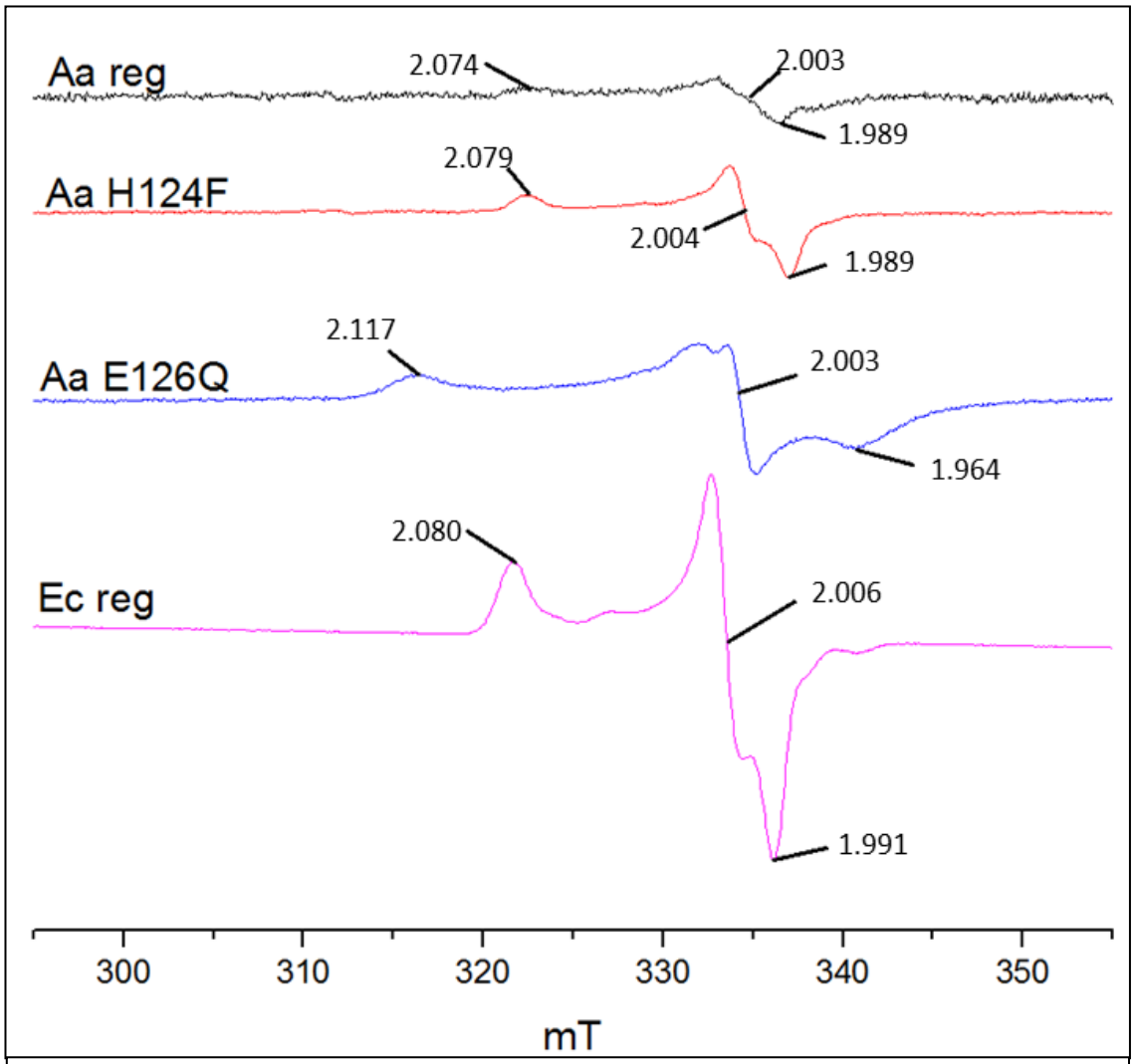

Figure 4-2 'Product' signal comparison.
Take from Figure3-8, 9, 10, 11, respectively.

Comparison of a IPP induced signal reported by the Oldfield group with our 'product' signals show that there is limited similarities between the two types of signals (Fig. 4-3). The reduced IspH enzyme was incubated with the product IPP. The spectrum is shown in Figure 4-3 bottom trace. This signal was measured, however, at 6 K and also part of the reduced cluster is still detectable making it difficult to see the whole IPP-induced signal. The low-field peak, however, can be found at identical positions in both type of EPR signals which would be in line with the product signal being the IPP-induced signal. Efforts are underway to synthesize IPP so we can makthis paramagnetic species ourselves and measure it under the proper EPR conditions of temperature and power to confirm this assignment.

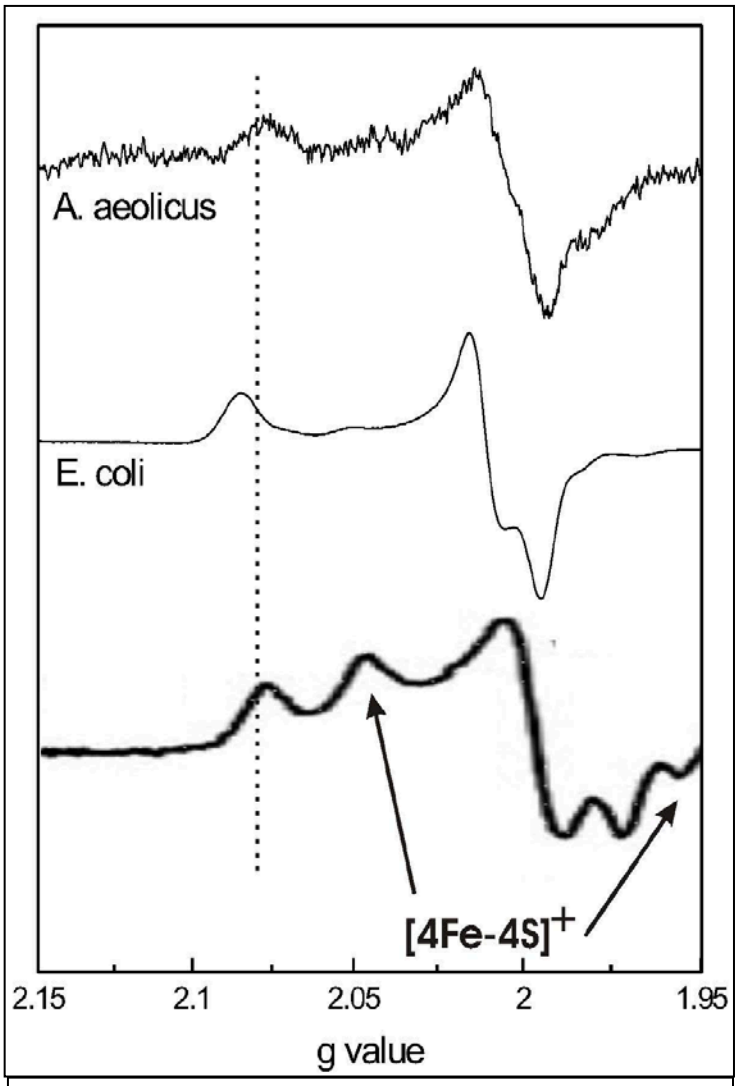

Figure 4-3 Product signal comparison

4.2.2.3 Overview of the different experiments

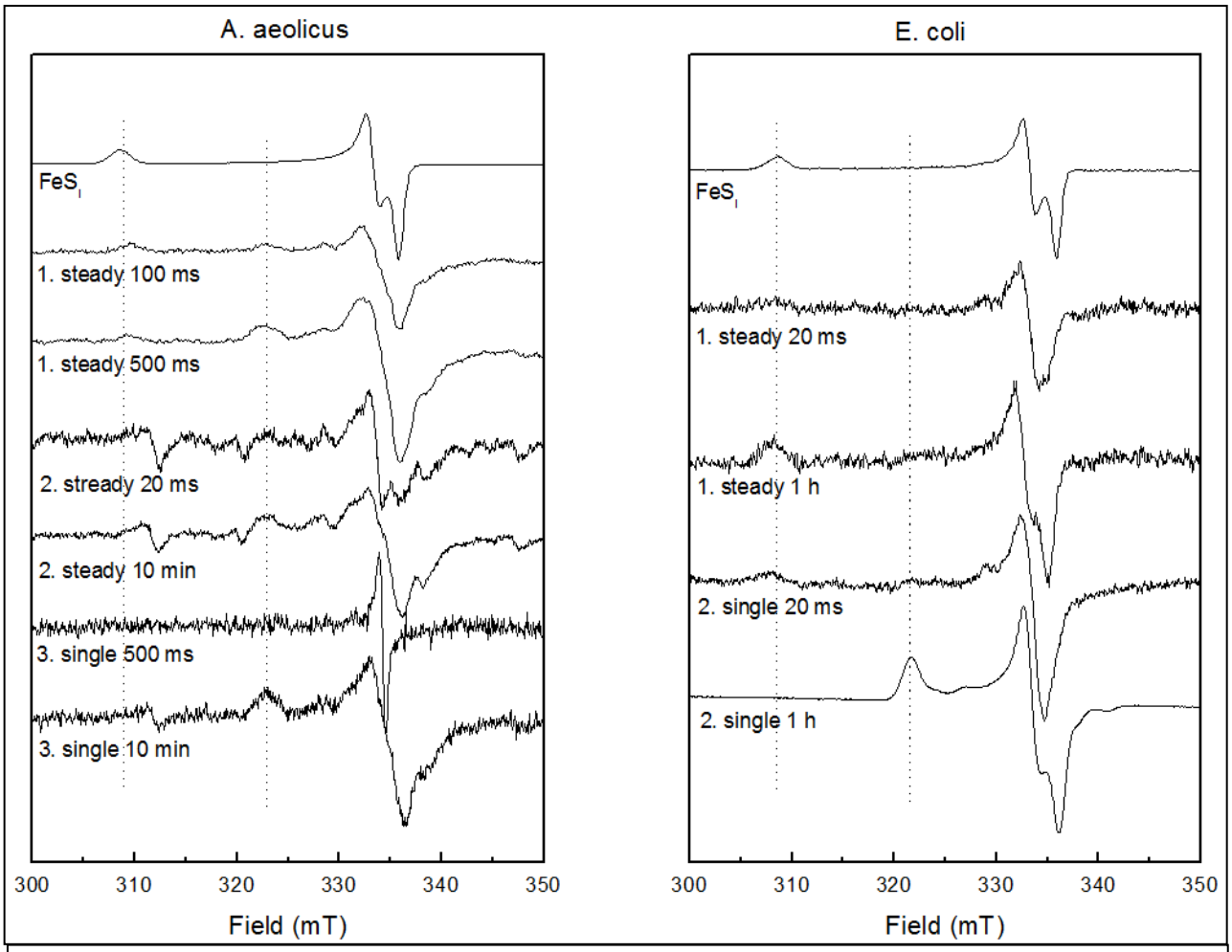

Figure 4-3 Overview of IspH WT from *A.aeolicus* and *E.coli*.
The data for *A.aeolicus* are adapted from Figure 3-5, 6, 8.
The data for *E.coli* are adapted from Figure 3-7, 11.

IspH from *E. coli* not only gave the best iron-sulfur cluster content, but also showed a well clued EPR signal pattern in single-turn-over experiments. A clear FeS_I signal with g-values of 2.176, 2.008, and 2.000 was present at 4.6ms. The signal intensity decreased significantly after 5-10s, but did not disappear completely after 6 minute. A clear product-like signal with g-values of 2.080, 2.006 and 1.991 was detectable, which stays detectable in sample prepared with a reaction time up to 60 min. We assign this signal to rebinding of product to the reduced cluster.

This assignment is important since it is also detected in some of the other experiments even when the FeSI signal is not detected. Therefore we have to assume that is some of the experiments the intensity of the formed FeSI species is just too low to pick out in the noise. From Figure 4-3 another trend can be detected. The FeS_I signal was detectable in the WT IspH from *A. aeolicus* when 5 mM HMBPP was used (Fig 4-3, left panel '1 steady 100 ms'). When 1.5 mM was used no FeS_I was detected (Fig 4-3, left panel '2 steady 20 ms'). Similarly when 150 μM was used in the single-turn-over experiment (Fig. 4-3, left panel '3 single 500 ms'). The reason that the FeS_I signal is absent in some of the experiments (although it should be there due to the possible product formation) can be due to both low signal intensity of the signal due to low sample concentration and cluster content, but it could also be an effect of the HMBPP concentration. Although these concentrations are much higher than the K_M values the protein concentrations are also very high and the relative concentrations could be too close and prevent the ES complex formation in large amounts.

4.3. Future Experiments

(1) Kinetic parameters with dithionite as reductant

With the aim of finding the true reaction time - the actual product formation time - extra NMR measurement or mass spectroscopy experiments are needed to detect the actual product formation. IPP and DMAPP formation can be easily detected using both methods. LC-MS has been successfully used before in the detected of both substrates. This way the kinetic parameters can be obtained in the absence of methyl viologen.

(2) Protein inactivation

Although the rapid freeze-quench experiments is a straight forward and has been successfully performed with other enzymes, still some factors might interfere with the reaction. For example: a) the sensitivity of the protein to isopentane; b) The presence of high amounts of dithionite could cause cluster breakdown. The sensitivity of IspH to both should be tested.

(3) Intermediate determination

The charge of each iron in the cluster can be determined by Mössbauer measurements,. This requires the amount of ^{57}Fe labeled paramagnetic species to be higher than over 1mM, and our measurements show that this can easily be achieved. This method can help us to fully understand the charge of every iron atom on the iron-sulfur cluster for each intermediate.

These experiments will be done by Selamawit Ghebreamlak in the short future.

References

1. Zhao et al. Methylerythritol phosphate pathway of isoprenoid biosynthesis. Annu Rev Biochem (2013) vol. 82 pp. 497-530 (for everything)
2. Shiao et al. The purification and properties of a protein kinase and the partial purification of a phosphoprotein phosphatase that inactivate and activate acetyl-CoA carboxylase. Biochem Biophys Res Commun (1981) vol. 98 (1) pp. 80-7
3. Qureshi et al. 3-hydroxy-3-methylglutaryl-CoA reductase from yeast. Meth Enzymol (1981) vol. 71 Pt C pp. 455-61
4. Bloch. Sterol molecule: structure, biosynthesis, and function. Steroids (1992) vol. 57 (8) pp. 378-83
5. Rohmer et al. Isoprenoid biosynthesis in bacteria: a novel pathway for the early steps leading to isopentenyl diphosphate. Biochem J (1993) vol. 295 (Pt 2) pp. 517-24
6. Rohmer. The discovery of a mevalonate-independent pathway for isoprenoid biosynthesis in bacteria, algae and higher plants. Nat Prod Rep (1999) vol. 16 (5) pp. 565-74
7. Eisenreich et al. Biosynthesis of isoprenoids via the non-mevalonate pathway. Cell Mol Life Sci (2004) vol. 61 (12) pp. 1401-26
8. Gräwert et al. Reductive dehydroxylation of allyl alcohols by IspH protein. Angew Chem Int Ed Engl (2010) vol. 49 (47) pp. 8802-9

9. Gräwert et al. Probing the reaction mechanism of IspH protein by x-ray structure analysis. Proc Natl Acad Sci USA (2010) vol. 107 (3) pp. 1077-81
10. Span et al. Structures of Fluoro, Amino, and Thiol Inhibitors Bound to the [Fe(4) S(4)] Protein IspH. Angew Chem Int Ed Engl (2013) vol. 52 (7) pp. 2118-21
11. Altincicek et al. LytB protein catalyzes the terminal step of the 2-C-methyl-D-erythritol-4-phosphate pathway of isoprenoid biosynthesis. FEBS Lett (2002) vol. 532 (3) pp. 437-40
12. Rekittke et al. Structure of (E)-4-hydroxy-3-methyl-but-2-enyl diphosphate reductase, the terminal enzyme of the non-mevalonate pathway. J Am Chem Soc (2008) vol. 130 (51) pp. 17206-7
13. Xu et al. A Closer Look at the Spectroscopic Properties of Possible Reaction Intermediates in Wild-Type and Mutant (E)-4-Hydroxy-3-methylbut-2-enyl Diphosphate Reductase. Biochemistry (2012) pp. (our lab)
14. Malkin and Rabinowitz. The reconstitution of clostridial ferredoxin. Biochem Biophys Res Commun (1966) vol. 23 (6) pp. 822-7
15. Zheng et al. Assembly of iron-sulfur clusters. Identification of an iscSUA-hscBA-fdx gene cluster from Azotobacter vinelandii. J Biol Chem (1998) vol. 273 (21) pp. 13264-72
16. Beinert et al. Iron-sulfur clusters: nature's modular, multipurpose structures. Science (1997) vol. 277 (5326) pp. 653-9
17. Meyer. Iron-sulfur protein folds, iron-sulfur chemistry, and evolution. J Biol Inorg Chem (2008) vol. 13 (2) pp. 157-70
18. Booker et al. Self-sacrifice in radical S-adenosylmethionine proteins. Curr Opin Chem Biol (2007) vol. 11 (5) pp. 543-52

19. Lill. Function and biogenesis of iron-sulphur proteins. Nature (2009) vol. 460 (7257) pp. 831-8

20. Johnson et al. Structure, function, and formation of biological iron-sulfur clusters. Annu Rev Biochem (2005) vol. 74 pp. 247-81

21. Unciuleac et al. In vitro activation of apo-aconitase using a [4Fe-4S] cluster-loaded form of the IscU [Fe-S] cluster scaffolding protein. Biochemistry (2007) vol. 46 (23) pp. 6812-21

22. Py et al. Fe-S clusters, fragile sentinels of the cell. Curr Opin Microbiol (2011) vol. 14 (2) pp. 218-23

23. Ranquet et al. Cobalt stress in Escherichia coli. The effect on the iron-sulfur proteins. J Biol Chem (2007) vol. 282 (42) pp. 30442-51

24. Chillappagari et al. Copper stress affects iron homeostasis by destabilizing iron-sulfur cluster formation in Bacillus subtilis. J Bacteriol (2010) vol. 192 (10) pp. 2512-24

25. Shimomura et al. Characterization and crystallization of an IscU-type scaffold protein with bound [2Fe-2S] cluster from the hyperthermophile, aquifex aeolicus. J Biochem (2007) vol. 142 (5) pp. 577-86

26. Agar et al. IscU as a scaffold for iron-sulfur cluster biosynthesis: sequential assembly of [2Fe-2S] and [4Fe-4S] clusters in IscU. Biochemistry (2000) vol. 39 (27) pp. 7856-62

27. Loiseau et al. ErpA, an iron sulfur (Fe S) protein of the A-type essential for respiratory metabolism in Escherichia coli. Proc Natl Acad Sci USA (2007) vol. 104 (34) pp. 13626-31

28. Wang et al. Bioorganometallic mechanism of action, and inhibition, of IspH. Proc Natl Acad Sci USA (2010) vol. 107 (10) pp. 4522-7

29. Wang et al. Are free radicals involved in IspH catalysis? An EPR and crystallographic investigation. J Am Chem Soc (2012) vol. 134 (27) pp. 11225-34

30. Hecht, S et al. Studies on the non-mevalonate isoprenoid biosynthetic pathway. Simple methods for preparation of isotope-labeled (E)-1-hydroxy-2-methylbut-2-enyl 4-diphosphate. Tetrahedron Lett. (2002) 43, 8929 – 8933.

31. Andrew B et al. Trisammonium geranyl diphosphate. Organic Syntheses, Coll. (1988) Vol. 8, p.616 (1993); Vol. 66, p.211.

32. Hagen. EPR spectroscopy as a probe of metal centres in biological systems. Dalton Trans (2006) (37) pp. 4415-34

33. Marina Brustolon (2009). Electron paramagnetic resonance: a practitioner's toolkit. John Wiley and Sons. p. 3. ISBN 0-470-25882-9.